Highlights of Joint Research

Synchrotron Radiation Laboratory

The Synchrotron Radiation Laboratory (SRL) was established in 1975 as a research group dedicating to solid state physics using synchrotron radiation. In 1989, the SRL started to hold the Tsukuba branch, a branch laboratory in the Photon Factory (PF), High Energy Accelerator Research Organization (KEK). The SRL consists of the accelerator physics group and the solid state spectroscopy group. The members of the accelerator group have been carrying out research works on the accelerator physics and developing various new accelerator related technology in collaboration with other SR facilities. The spectroscopy group has been not only serving users at the Tsukuba branch with technical supports and advices, but also carrying out their own research works on advanced solid state spectroscopy. SRL maintains an undulator called Revolver, two beamlines and three experimental stations; BL-18A for angle-resolved photoemission spectroscopy and undulator beamlines, BL-19A and BL-19B, for spin-resolved photoelectron spectroscopy and soft X-ray emission spectroscopy experiments, respectively. They are fully opened to outside users for experiments using high brilliant synchrotron radiation from the undulator. The operation time of these beamlines are about 4000 hours and the number of users is more than 100 a year.

In 2007, two new apparatuses have been opened to the users. They are SCIENTA SES100 energy analyser at BL-18A and VLEED spin detector at BL19A. The new apparatuses are utilized in angle-resolved and spin-resolved photoemission experiments with higher energy- and momentum-resolutions. Recently, our VLEED system showed the best efficiency of this kind of spin detector (see the highlight in this volume).

The staff members of SRL, the solid state spectroscopy group, participate to the Materials Research Division of the Synchrotron Radiation Research Organization of the University of Tokyo (SRRO). They play essential roles in promoting scientific activities using SR and started to construct a new 25m-long undulator and beamline at the SPring-8. The beamline will be equipped with experimental apparatuses using high brilliance synchrotron radiation in soft X-ray region. They are those for time-resolved experiments and nano-materials research experiments, which will only be possible using third generation light source and will promise us a considerable progress in the studies of nano-particles and real time observation of magnetic domains and of chemical reactions at catalytic surfaces, etc.

The new undulator arrived at SPring-8

The accelerator group designed and started to construct the new 25-m undulator of the University of Tokyo at SPring-8 in collaboration with the SPring-8 ID group. The new undulator consists of four horizontal and four vertical figure-8 undulator segments and seven phase shifters between the segments and can provide not only horizontally- and vertically-polarized radiations but also circularly-polarized radiation with fast helicity switching. The four horizontal figure-8 undulator segments were already constructed and a prototype of the electromagnetic phase shifter was designed and fabricated. A pulsed sextupole magnet was developed to reduce the stored beam oscillation at top-up injection and installed in the PF-ring and a digital beam position monitor system was upgraded and its performance test was successfully carried out at ISSP and the KEK-ATF damping ring. The accelerator group also studied future ERL(energy recovery linac) light sources and developed ERL components. Exact resistive-wall wake function of a vacuum pipe was calculated to simulate the multi-bunch beam motion due to the resistive-wall wake in an ERL. Center and end single-cell superconducting cavities were fabricated and tested in collaboration with KEK and JAEA and their acceleration fields of higher than 15 MV/m were achieved. A nine-cell cavity and two ceramic windows for the input coupler were also fabricated and will be tested. Furthermore a fiber laser oscillator for driving an ERL photocathode gun was developed in collaboration with AIST and KEK.

Neutron Science Laboratory

The Neutron Science Laboratory (NSL) has been playing a central role in neutron scattering activities in Japan since 1961 by performing its own research programs as well as providing a strong general user program for the university-owned various neutron scattering spectrometers installed at the JRR-3 operated by Japan Atomic Energy Agency in Tokai. In 2003, the Neutron Scattering Laboratory was reorganized as the Neutron Science Laboratory to further promote the neutron science with use of the instruments in JRR-3. Under the general user program supported by NSL, 14 university-group-owned spectrometers in the JRR-3 reactor (20MW) are available for a wide scope of researches on material science, and proposals close to 300 are

Fig. 1. The reactor hall of JRR-3. The eight neutron scattering instruments are attached to the horizontal beam tubes in the reactor experimental hall. Two thermal and three cold guides are extracted from the reactor core towards the guide hall located to the left.

submitted each year, and the number of visiting users under this program reaches over 6000 person-day/year.

Triple axis spectrometers and a high resolution powder diffractometer are utilized for a conventional solid state physics and a variety of research fields on hard-condensed matter, while in the field of soft-condensed matter science, researches are mostly carried out by using the small angle neutron scattering (SANS-U) and/or neutron spin echo (iNSE) instruments. The upgraded time-of-flight (TOF) inelastic scattering spectrometer is also available through the ISSP-NSL user program.

Major research topics on the hard-condensed matter science cover stripe order in high-T_c superconductors, and closely related 2 dimensional systems, charge and orbital ordering in CMR manganites, quadrapolar ordering in rare-earth based intermetallic compounds, spin dynamics of low dimensional dimmer systems, etc. On the other hand, the research topics on the soft-condensed matter science cover structural characterization of polymer blends, micelles, amphiphilic polymers block copolymers, liquid crystals, proteins, inorganic gels, dynamics of brush-polymers on surface, slow dynamics of surfactants, pressure dependence of dynamics of amphiphilic membranes, and so on. In addition, there are a variety of activities on fundamental physics, neutron beam optics, developments of neutron scattering techniques.

The NSL also operates the U.S.-Japan cooperative program on neutron scattering, providing further research opportunities to material scientists who utilize the neutron scattering technique for their research interests.

The details of individual studies and research highlights in JFY2006 are reported in the NSL-ISSP Activity Report vol. 14.

Supercomputer Center

The Supercomputer Center (SCC) is a part of the Materials Design and Characterization Laboratory (MDCL) of ISSP. Its mission is to serve the whole community of computational condensed-matter physics of Japan providing it with high performance computing environment. In particular, the SCC selectively promotes and supports large-scale computations. For this purpose, the SCC invites proposals for supercomputer-aided research projects and hosts the Steering Committee, as mentioned below, to evaluate the proposals.

The SCC operates two super-computers, systems A and B, which were renewed in March 2005. System A is Hitachi SR11000/48 that consists of 48 high performance nodes composed of tightly-coupled microprocessors. With the aid of the automatic parallelization of FORTRAN compiler, a node of System A can be used as if it were a single-processor computer. System A has 2.8TB memory and achieves 5.8 TFlops peak performance in total. On the other hand, System B, which is SGI Altix 3700/1280, is a parallel supercomputer with relatively loose coupling. It consists of 19 nodes inter-connected by a gigabit Ethernet network. Each node is a distributed-shared-memory-type computer consisting of 64 Intel Itanium 2 CPUs interconnected by a rather high performance network and have 64 GB memory. System B achieves 7.7 TFlops total throughput performance.

All staff members of university faculties or public research institutes in Japan are invited to propose research projects (called User Programs). The proposals are evaluated by the Steering Committee of SCC. Pre-reviewing is done by the Supercomputer Project Advisory Committee. In fiscal year 2007 totally 184 projects were approved. The total points applied and approved are listed in Table. 1 below.

The research projects are roughly classified into the following three (together with the number of approved projects):

First-Principles Calculation of Materials Properties (67)
Strongly Correlated Quantum Systems (49)
Cooperative Phenomena in Complex, Macroscopic Systems (68)

All the three involve both methodology of computation and its applications. The results of the projects are reported in 'Activity Report 2007' of the SCC. Every year typically four projects are selected for invited papers, which appear at the beggining of the Activity Report. In the Activity Report 2007, the following four invited papers are included:

"Gaussian-Basis Monte Carlo Studies on Two Dimensional Hubbard Model", by Takeshi AIMI, Daisuke TAHARA and Masatoshi IMADA
"First-Principles Study of Multiferroic Oxides" by Tamio OGUCHI
"Hydration Effect on Temperature Dependence of Protein Dynamics Studied by Molecular Dynamics Simulation of Crystalline Protein" by Yasumasa JOTI and Akio KITAO
"Quantum Phase Transitions to VBS States" by Naoki KAWASHIMA and Kenji HARADA

Class	Max/Min Points	Application	Number of Projects	Total Points			
				Applied		Approved	
				System A	System B	System A	System B
A	<100K	any time	8	470K	330K	470K	330K
B	<2M	twice a year	42	57.4M	25.1M	54.7M	22.3M
C	<20M	twice a year	117	1117M	852M	1002M	715M
D		any time	16	194M	271M	166M	216M
S	>20M	twice a year	1	50M	0	50M	0
Total			184	1419M	1148M	1273M	954M

Table 1. Research projects approved in 2007. The maximum points allotted to the project of each class are the sum of the points for the two systems; 1 K point of System-A corresponds to charge for 0.37 hours × node, while 1K point is 0.22 hours × 64CPU for System-B.

International MegaGauss Science Laboratory

The aim of this laboratory is to study the physical properties of solid-state materials (such as semiconductors, magnetic materials, metals, insulators, superconducting materials) under ultra-high magnetic field conditions. Such a high magnetic field is also used for controlling the new material phase and functions. Our pulse magnets, at moment, can generate up to 85 Tesla by non-destructive manner, and from 100 up to 850 Tesla (the world strongest as an in-door record) by destructive (the single turn coil and the electro-magnetic flux compression) methods.

They are opened for scientists both from Japan and from overseas, especially from Asian countries, and many fruitful results are expected to come out not only from collaborative research but also from our in-house activities. One of our ultimate goals is to provide the scientific users as our joint research with magnets capable of a 100 T, milli-second pulses in a non-destructive mode, and to offer versatile physical precision measurements. The available measuring techniques now involve magneto-optical measurements, cyclotron resonance, spin resonance, magnetization and transport measurements.

Our interests cover the study on quantum phase transitions (QPT) induced by high magnetic fields. Field-induced QPT has been explored in various materials such as quantum spin systems, strongly correlated electron systems and other magnetic materials. Non-destructive strong pulse magnets are expected to provide us with reliable and precise solid state physics measurements. The number of collaborative groups for the research is over 50 in the year of 2007. Multiple extreme physical conditions combined with ultra-low temperatures and ultra-high pressures are also available.

A 210 MJ flywheel generator which is the world largest DC power supply (recorded in Guinness book of records in 1907/98) has been installed in the newly build DC Flywheel generator station at our Institute. The generator, once disassembled from the one used for Toroidal magnetic field coil in JFT-2M (JAERI Fusion Torus-2M) Tokamak nuclear fusion testing device, is now renewed as a power supply for the pulse magnets. The construction of the magnet service station has also been accomplished. The magnet technologies are intensively devoted to the quasi-steady long pulse magnet (an order of 1-10 sec) energized by the giant DC power supply, and also used for the outer-magnet coil to realize a 100 Tesla nondestructive magnet.

Our destructive magnets, such as the single-turn coil and the electro-magnetic flux compression (EMFC) systems, would be oriented toward easier access and more reliable measurements for solid-state physics than previously obtainable. One of our recent successes was the achievement of over 850 T within a 4 MJ energy injection by the EMFC, in which a new type of primary coil with a simpler design was employed. These are oriented for developing new horizons in material science realized under such extreme quantum limit conditions.

Fig. 1. The building for the flywheel generator (right hand side) and a long pulse magnet station (left hand side). The flywheel giant DC generator is 350 ton in weight and 5 m high (bottom). The generator, capable of a 51 mega watt out put power with a 210 mega joule energy storage, is planned to energize the long pulse magnet generating 100 Tesla without destruction.

Low Energy Excitations in the Vortex State of the Anisotropic s-Wave Superconductor $CeRu_2$

K. Machida and T. Sakakibara

It is now well established that zero energy density of states (ZEDOS) in the vortex state of *d*-wave superconductors (SCs) exhibit a characteristic oscillation as a function of the angle between the magnetic field H and the nodal directions, due to the "Doppler effect" of nodal quasiparticles [1,2] This ZEDOS oscillation, which can be observed by specific heat $C(H)$ and thermal conductivity measurements in rotating H, provides a means to determine the gap structures of nodal SCs.

Here we demonstrate that the field rotation experiments can also be a powerful tool to examine the gap structure of anisotropic *s*-wave SCs, where the gap amplitude only modulates on the Fermi surface and does not vanish. The system we studied is a cubic Laves phase compound $CeRu_2$ with the superconducting transition temperature T_c of 6.3 K and the upper critical field H_{c2} of 5.2 T [3]. Figure 1 shows the experimental results. When H is rotated in a (001) plane, we observed a clear fourfold oscillation in $C(H)$ (upper panel), which can be expressed in the form:

$$C(H,\theta)=C_0+C_H(1+A_4\cos 4\theta),$$

where C_0 and C_H denote the field-independent and dependent parts of the specific heat, respectively. θ is the field angle measured from [100]. The coefficient A_4 is the relative amplitude of the fourfold oscillation, which is strongly H and T dependent as shown in the contour plot in the lower panel. It should be noticed that A_4 takes the maximum at finite H, and rapidly diminishes by decreasing H at T=0.34 K or decreasing T at H=0.5 T.

We have performed microscopic calculations by solving the Eilenberger equations fully self-consistently assuming the gap function:

$$\Delta(\boldsymbol{k})= \Delta_0(1+\alpha\cos 4\theta),$$

where the gap anisotropy parameter α is chosen to be

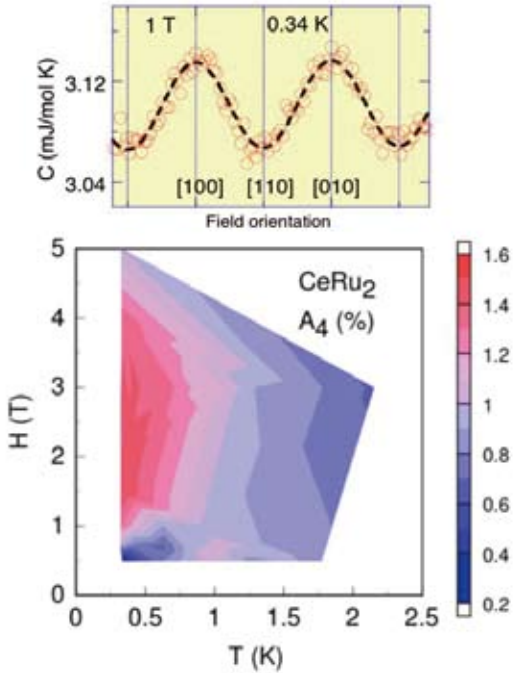

Fig. 1. Angular oscillation of the specific heat in the vortex state of $CeRu_2$ when H is rotated in the (001) plane (upper panel), and a contour plot of the T and H variation of the fourfold amplitude A_4.

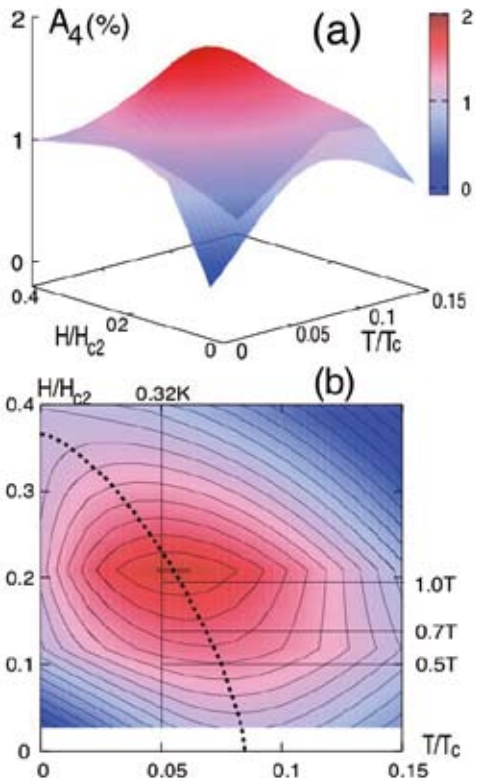

Fig. 2. Landscape of $A_4(T,H)$ calculated for the anisotropic *s*-wave model with α=0.5. (a) Stereographic view and (b) contour plot.

0.5 to best reproduce the experimental data. Figure 2 shows the results of $A_4(T,H)$, where the upper panel (a) is a stereographic view and the lower panel (b) displays a contour plot. It can be seen clearly that the maximum of A_4 is located at *finite* T and H. This feature is absent in the nodal gap SCs where the landscape in $A_4(T,H)$ is a simple peak structure with the maximum located at T=0 and H=0. The present result is fully understandable because in anisotropic *s*-wave SCs a finite minimum gap Δ_{min} exists and is overcome either by an applied field or by thermal excitations. Our calculations confirm that $CeRu_2$ is an aisotropic *s*-wave SC having the gap anisotropy ratio $\Delta_{min}/\Delta_{max}$~0.3 with Δ_{min} located along [110] directions [3].

References

[1] I. Vekhter *et al.*, Phys. Rev. B **59**, R9023 (1999).
[2] P. Miranovic, M. Ichioka, K. Machida, and N. Nakai, J. Phys. Condens. Matter **17**, 7971 (2005).
[3] A. Yamada, T. Sakakibara, J. Custers, M. Hedo, Y. Onuki, P. Miranovic, and K. Machida, J. Phys. Soc. Jpn. **76** 123704 (2007).

Authors

A. Yamada, T. Sakakibara, J. Custers, M. Hedo[a], Y. Onuki[b], P. Miranovic[c], and K. Machida[d]
[a]University of Ryukyu
[b]Osaka University
[c]University of Montenegro
[d]Okayama University

Ground State in One-Dimensional Molecular Conductor Exhibiting Giant Magnetoresistance

N. Hanasaki and H. Tajima

The gigantic response of the spin-dependent transport has made many important contributions to physics and been applied to magnetic storage. For the realization of the

giant magnetoresistance, the intermolecular or intramolecular interaction between the conduction electron and the local moments is indispensable. In case of the intermolecular interaction between the molecules contributing to the conduction and the other molecules having the local moments, it is necessary to control the molecular arrangement precisely in the crystal. The metal-phthalocyanine molecule is advantageous, since it provides the strong intramolecular interaction. Figure 1(a) shows the structure of the $Fe(Pc)(CN)_2$ (Pc=phthalocyanine) molecule. This molecule has the local moment in the next HOMO (HOMO=highest occupied molecular orbital), which reflects the *d*-orbital of the central Fe atom (red). HOMO consists of the atomic orbitals of the Pc planar molecule. As displayed in Fig.1(b) [1], in the crystal, the $Fe(Pc)(CN)_2$ molecules stack along the *c* axis. This molecular overlap provides the one-dimensional conduction band along the *c* axis.

In $TPP[Fe(Pc)(CN)_2]_2$ (TPP = tetraphenylphosphonium), the giant negative magnetoersistance is observed below 50K, where the resistance increases with lowering the temperature [2]. It is important to clarify the origin of the low-temperature insulating state. In order to investigate the charge state in the ground state, we measured the X-ray diffraction. Figure 2(a) shows the picture of the diffraction at 6K. Here, the X-ray beam energy and the oscillation angle were 20keV and 1 (degree), respectively. The vertical direction in Fig.2(a) is nearly parallel to the *c* axis, which is the one-dimensional conducting direction. Many spots existing along the direction perpendicular to the *c* axis correspond to the Bragg peaks. Besides these peaks, one can find the diffuse streak in the middle position between these lines of the Bragg peaks, as indicated by the arrows. This diffuse streak extends along the direction perpendicular to the *c* axis. The intensity of these diffuse streaks is six orders of magnitude smaller than that of the Bragg peaks. We display the intensity of this diffuse streak as a function of the position (pixels) along the *c* axis, in Fig.2(b). The intensity increases with lowering the temperature. This intensity enhancement coincides with the low-temperature enhancement of the resistance and the Seebeck effect [1]. Thus, this diffuse streak is related to the mechanism of the insulating ground state. Taking into account the three-quarter-filled conduction band in $TPP[Fe(Pc)(CN)_2]_2$ and the periodicity of 2 X *c* of the diffuse streak, the nearest neighbor Coulomb interaction *V* is responsible for the insulating state. The crystal structure analysis at 30K suggests no dimerization of the Pc molecules. The ^{57}Co nuclear quadrapole resonance (the joint research with Takigawa Lab.) in the isostructural compound $TPP[Co(Pc)(CN)_2]_2$ reveals the very weak charge disproportionate state [3]. Thus, it is reasonable to consider

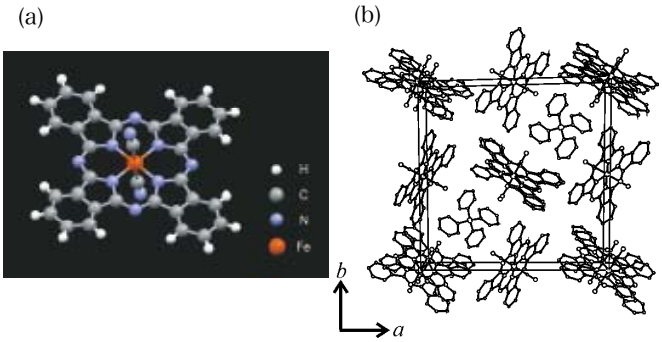

Fig. 1. (a) Structure of the $Fe(Pc)(CN)_2$ molecule. The central Fe atom (red) has the coordination to the Pc planar molecule and the CN ligands. (b) Crystal structure of $TPP[Fe(Pc)(CN)_2]_2$ viewed from the *c* axis [1].

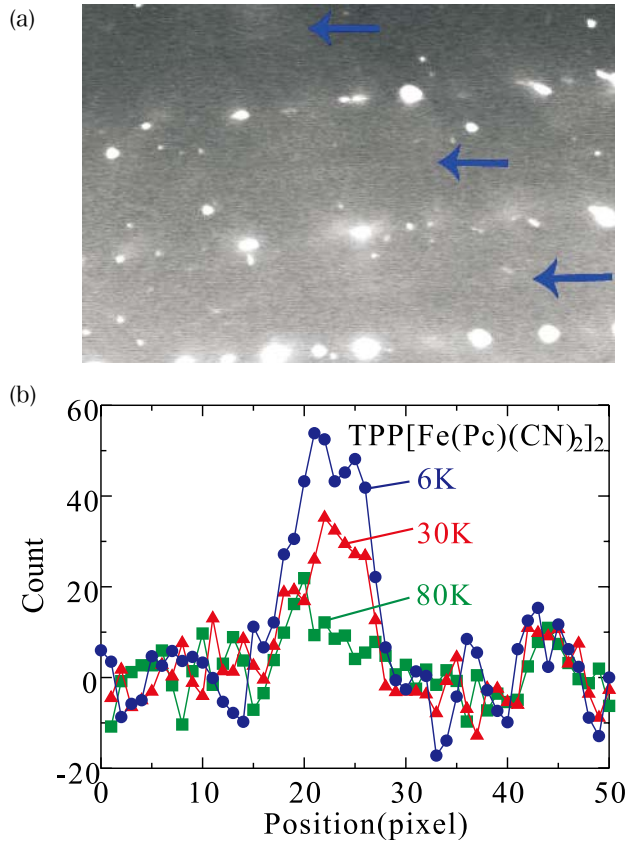

Fig. 2. (a) X-ray diffraction pattern in one-dimensional molecular conductor $TPP[Fe(Pc)(CN)_2]_2$. The $4k_F$ diffuse streak is observed in the positions indicated by the arrows. (b) Intensity of the $4k_F$ diffuse streak in the central arrow in Fig.2(a) plotted as a function of the position (pixels) along the c axis.

that the diffuse streak is ascribed to the charge disproportionation (the weak charge order).

Recently, we also observed the enhancement of the dielectric constants by applying the magnetic field at the low temperatures, where the diffuse streak is observed, suggesting the magnetic-field-induced melting of the charge disproportionation, which is a possible origin of the giant negative magnetoresistance.

References

[1] M.Matsuda *et al.*, J. Mater. Chem. **10**, 631 (2000).
[2] N.Hanasaki *et al.*, J. Phys. Soc. Jpn. **75**, 033703 (2006).
[3] N.Hanasaki *et al.*, J. Phys. Soc. Jpn. **75**, 104713 (2006).

Authors

N. Hanasaki[a], M. Matsuda, H. Tajima, M. Tanabe[a], Y. Nogami[a], and T. Inabe[b]
[a] Dept. of Physics, Okayama University
[b] Div. of Chemistry, Hokkaido University

Accurate Theoretical Evaluation of Raman Frequency Shift as a Pressure Gauge in Diamond Anvil Cell

R. Maezono

Diamond anvil cells are used to study condensed matter over a wide range of pressures and temperatures. The range of static pressures attainable today extends at least as far as the conditions prevailing in the center of the earth (>360 GPa). A thorough understanding of the physical properties of diamond at high pressure is of great importance in the design and operation of such cells, but although there

have been many experimental studies of this material, some properties, including the equation of state, remain imperfectly characterized.

The equation of state (EOS) can be described over a wide range of pressures in terms of the zero-pressure values of the equilibrium volume, the isothermal bulk modulus, and its pressure derivative. The values of the volume and bulk modulus for diamond are well established experimentally over a substantial range of temperatures, but there is considerable uncertainty about the pressure derivative of bulk modulus. A recent study [2] gave 3.0(1) for the derivative at room temperature, although it has been argued that the ruby luminescence pressure calibration used in the analysis of the experimental data should be revised [3]. The most commonly cited experimental value [4] is 4.0(5), but the error bar on this result leads to considerable uncertainty in the EOS at high pressures.

Diamond is highly transparent to electromagnetic radiation over a large range of wavelengths, and the sample within a diamond anvil cell may be examined in situ under elevated pressure by X-ray diffraction techniques and also by Raman, Brillouin, and infrared spectroscopies. The Raman technique in particular has been used extensively to study the threefold-degenerate zone-center optical phonon mode of diamond under pressure. It has been suggested [2] that the volume dependence of the Raman frequency could be used as a pressure gauge in diamond diamond anvil cell experiments, and more information about the Raman frequency under high compression would help in the calibration process.

In view of the unsatisfactory situation regarding our knowledge of the EOS of diamond and the importance of the material, we believe that a study using highly accurate continuum quantum Monte Carlo (QMC) techniques would be useful. We have therefore calculated the EOS up to a pressure of about 500 GPa and the Raman frequency of diamond up to about 320 GPa using both the variational and diffusion quantum Monte Carlo (VMC and DMC) techniques.

Vinet EOS is used to estimate parameters in EOS, which has been demonstrated to work well over large pressure ranges. The values of equilibrium volume and bulk modulus obtained from the DMC calculations are the closest of the theoretical values to experiment. The value of the derivative is estimated as 3.7(1) using DMC. Given the level of agreement between the various theoretical methods including DFT it seems that the experimental value of 3.0(1) cannot be sustained. Our QMC results are thus consistent with the ideas of Holzapfel [3] regarding the refinement of the ruby luminescence pressure scale used in analyzing diamond anvil data.

We computed the frequency of the first-order Raman mode of diamond at four volumes corresponding to a pressure range of approximately 0–320 GPa using the frozen phonon method. The volume dependence of the Raman frequency by our QMC predicts the Gruneisen parameter to be 0.94(1), providing a gauge to measure high pressure by a reliable theoretical evaluation.

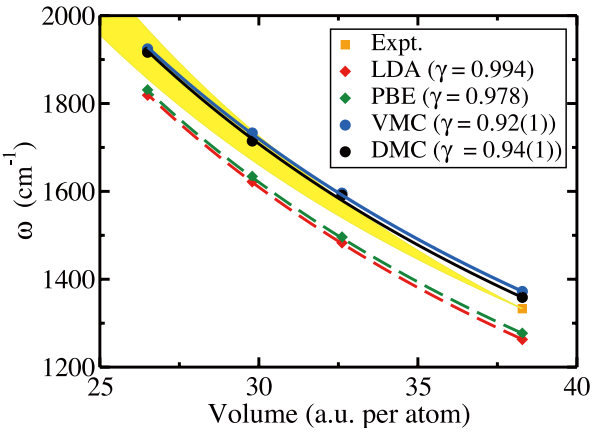

Fig. 1. The Raman frequency as a function of volume. The shaded yellow region shows the range of values obtained by using Gruneisen parameters in the range 0.9-1.06.

References

[1] R. Maezono, A. Ma, M. D. Towler, and R. J. Needs, Phys. Rev. Lett. **98**, 025701 (2007).
[2] F. Occelli, P. Loubeyre, and R. LeToullec, Nat. Mater. **2**, 151 (2003).
[3] W. B. Holzapfel, J. Appl. Phys. **93**, 1813 (2003).
[4] H. J. McSkimin and P. Andreatch, Jr., J. Appl. Phys. **43**, 2944 (1972).

Author
R. Maezono
School of Information Science, Japan Advanced Institute of Science and Technology

Dynamic Nuclear Polarization in Corbino Geometry

M. Kawamura, T. Machida, and S. Katsumoto

Effect of nuclear spin polarization on the transport through semiconductor heterostructures is now attracting much attention. Especially dynamic nuclear polarization (DNP) due to some non-equilibrium phenomenon is an important candidate as a tool to manipulate nuclear spins quantum mechanically because it potentially polarizes spins with very high efficiency without external magnetic field. DNP occurs, for example, in the breakdown of quantum Hall states at high biasing currents, which is a limitation of accuracy in quantum Hall resistance standard. This is also very convenient for spin manipulation, in that the polarization can be readily detected through the conductance with extremely high sensitivity. In order for this method to be useful, we should clarify the location (in the samples) and the origin of DNP.

For the elimination of the possible edge channel originated non-equilibriums, we have adopted the Corbino geometry (the inset of Fig. 1(b)), where the voltage is applied radially across the two-dimensional electron system at an AlGaAs/GaAs hetero-interface and no edge channel exists in the sample. In Fig. 1, we fixed the external magnetic field at which the filling factor is 1.05 and swept the voltage across the sample. The breakdown occurs around 30 mV and above that we observe finite current and apparent hysteresis. The latter is due to DNP, which is evidenced by the response to applied radio frequency shown in the inset of Fig. 1(a). In the response, a current dip due to the magnetic resonance of ^{75}As nuclei is evident.

Now we performed a "pump and probe" experiment. In the procedure, the voltage was swept up to "pumping" voltage, where the system was kept for 900 s. Then the voltage was abruptly moved to "probing" voltage, which was fixed at 50 mV in the present experiment, and the transient current increase ΔI was measured. Figure 1(b) shows thus measured transient current as a function of the pumping

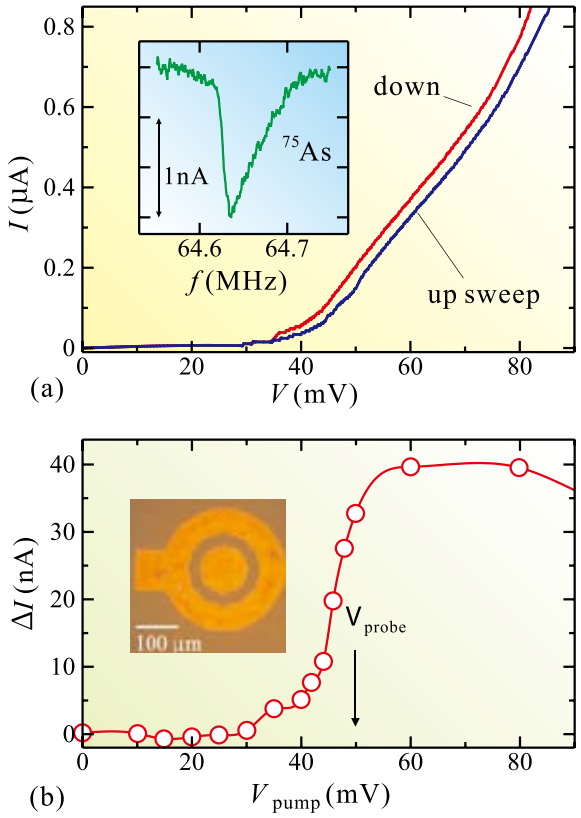

Fig. 1. (a) Device current as a function of the applied voltage. The blue and red curves correspond to up sweeping and down one, respectively. Apparent hysteresis is observed above 40 mV. The inset shows the current at 50 mV as a function of applied radio frequency. Strong dip due to ^{75}As nuclear magnetic resonance is observed. (b) Transient current as a function of pumping voltage. The probing voltage is fixed to 50 mV as indicated by the arrow. The inset shows a micrograph of the sample with the Corbino geometry.

voltage. The transient current steeply increases with the pumping voltage around 45 mV, which coincides with the rise of quantum Hall breakdown current.

The result indicates that the quantum Hall breakdown brings about the DNP. Since the breakdown is induced by the avalanche multiplication of electron-hole pairs due to inter-Landau level impact ionization, we deduce that the multiplication causes the DNP. In an odd-integer quantum Hall state, the avalanche kicks up electrons between different spin subbands, resulting in electron spin flips. The electron spin flips cause nuclear spin flips via hyperfine interaction. Our results demonstrate that such process occurs in bulk conductance channels and supports the above inference.

References

[1] M. Kawamura, H. Takahashi, S. Masubuchi, Y. Hashimoto, S. Katsumoto, K. Hamaya, and T. Machida, J. Phys. Soc. Jpn. **77**, 023710 (2008).

Authors

M. Kawamura[a], T. Machida[a], and S. Katsumoto

[a]Institute of Industrial Science, University of Tokyo

Fullerene Nanomesh on Nitrogen-modified Cu(001) Surface

F. Rosei, K. Sakamoto, and F. Komori

Controlled self-assembly of molecular nanostructures has been studied both for elucidating its mechanism in fundamental science and for possible future applications to devices, catalyses and so on. Among various methods for controlling self-assembly, the use of specific adsorbate-substrate interactions on template surfaces is a promising and general approach to guide the fabrication of large-scale inorganic or organic nanostructures. The use of surface cues to guide adsorption processes has been demonstrated on a variety of spontaneously nanostructured substrates. Ordered nanostructure arrays and thin films with distinct physical and chemical properties can be achieved on host templates by the site-specific nucleation of adsorbates and successive organized growth. In the present study, we use nanopatterns of the Cu(001)c(2×2)-N surfaces, which have been used as templates for the controlled growth of several metal-nanoisland arrays [1], for making periodic nano-assemblies of fullerene molecules.

A two-dimensional square lattice of nitrogen-adsorbed areas with a typical lateral dimension of roughly 5 nm [2] can be made when the average density of adsorbed nitrogen atoms on Cu(001) is 35% of that of the surface Cu atoms, as shown in Fig. 1(a). Narrow strips of the clean Cu surface periodically separate the nitrogen-adsorbed areas. Nitrogen atoms adsorb on the four-fold hollow site on the Cu(001) lattice, resulting in the Cu(001)c(2×2)-N phase which is imaged as depressed patches with sides running along <010> azimuth orientations.

Figure 1(b) shows the morphology after the deposition of ~ 0.08 ML C_{60} molecules onto the grid surface at RT. Here, 1 ML is defined as the coverage of the single molecular layer. As expected, the fullerenes tend to selectively adsorb on the clean Cu regions due to the relatively stronger interaction between C_{60} and Cu, at which charge transfers from substrate to C_{60}. No nucleation is observed for C_{60} at the c(2×2) surface. Thus, the preferential nucleation indicates weaker interaction of the molecule with the

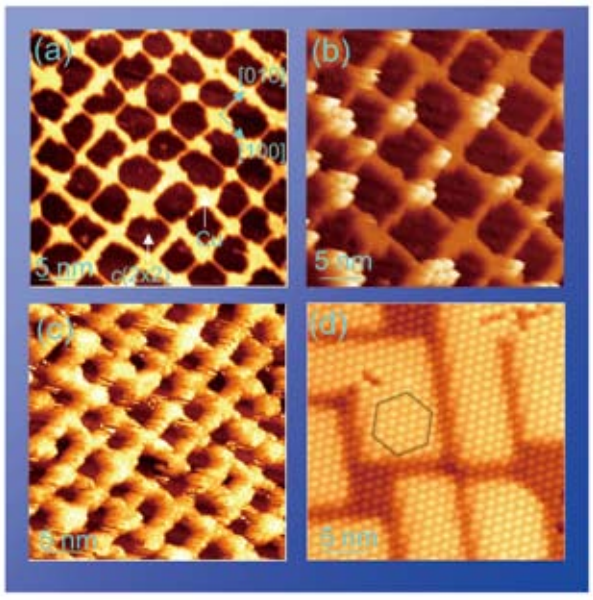

Fig. 1. STM images showing a N-adsorbed grid Cu(001) surface (a), nucleation of C_{60} molecules onto the grid surface at RT (b), C_{60} molecular nanomesh on the grid surface (c), and a single layer film of C_{60} on N-saturated Cu(001) surface with nanotrench structures(d). In (a), N-adsorbed square areas are imaged low, and separated by clean Cu surface, which is imaged high. Fullerenes first nucleate at wide and clean Cu areas (b), then cover the whole clean Cu surface (c), and finally make a single C_{60} layer on the grid surface of N-adsorbed and clean Cu areas with increasing the coverage. Fullerenes form a single molecular layer with maintaining the substrate nanostrucrures both on the grid and N-saturated (d) Cu(001) surfaces.

$c(2\times2)$-N surface than with the clean Cu surface. The deposited C_{60} can migrate freely on the $c(2\times2)$ area at RT. Selective nucleation on this nanopatterned surface has been previously reported for the deposition of various metals, and is expected to be a fairly general behavior [1].

An increase of C_{60} coverage to ~ 0.28 ML leads to the saturated adsorption of C_{60} on the clean Cu areas forming a 2D C_{60} molecular nanomesh with the single molecular layer height as shown in Fig. 1(c). This 2D nanomesh follows the grids of the template and thus is highly regular. Further deposition gives rise to the growth of C_{60} on the $c(2\times2)$-N surface until the first molecular layer is completed. The growth of C_{60} on this nanopatterned surface is different from metal growth on the same surface; in this case metal nanoislands grow up to 2 ML on the grid without wetting the $c(2\times2)$-N surface [1]. Further deposition of C_{60} results in the layer-by-layer growth of a C_{60} thin film.

On the N-saturated Cu(001) surface, C_{60} molecules grow also with a layer-by-layer mode keeping the substrate nanostructure as in Fig. 1(d). They thermally desorb at 400 K, and thus the interaction at the interface is a van der Waals force. The weak interface interaction can stabilize the substrate grid-nanopattern even after the multilayer growth of C_{60}. This is in contrast to the metal growth on the same surface, where nitrogen-atoms segregate to the surfaces of the deposited metal [3].

References

[1] F. Komori, S. Ohno, and K. Nakatsuji, Prog. in Surf. Sci. **77**, 1 (2004).
[2] F. M. Leibsle, C. F. J. Flipse, and A. W. Robinson, Phys. Rev. B **47**, 15865 (1993).
[3] D. Sekiba, S. Doi, K. Nakatsuji, and F. Komori, Surf. Sci. **590**, 138, (2005).

Authors

B. Lu, T. Iimori, K. Sakamoto[a], K. Nakatsuji, F. Rosei[b], and F. Komori,
[a]Graduate School of Advanced Integration Science, Chiba University
[b]INRS-EMT, University of Quebec

Resistance Switching in Oxide Heterostructures

I. Ohkubo and M. Lippmaa

Resistance switching in oxides is a phenomenon where the resistance of a material changes reversibly by the application of a large electric field. Depending on the type of material and the structure of a device, several different mechanisms can be at play, such as the formation of conducting filaments, modulating the height of a Schottky barrier, storing charge in trap states, etc. While resistance switching is at the heart of new nonvolatile memory development, it also highlights the need to understand the basic physical processes that govern the transport properties of nanoscale oxide layers, namely anion and cation diffusion, defect formation, and charge accumulation. Of special interest is how nonvolatile electronic or structural changes can be driven by electrostatic field.

One suitable material for resistance switching experiments is $Pr_{0.7}Ca_{0.3}MnO_3$ [1,2]. Earlier work has shown that the resistance change originates from the interface layer between the manganite film and an Aluminum electrode [3,4]. The basic switching structure is shown in Fig. 1, together with the time dependent resistance change

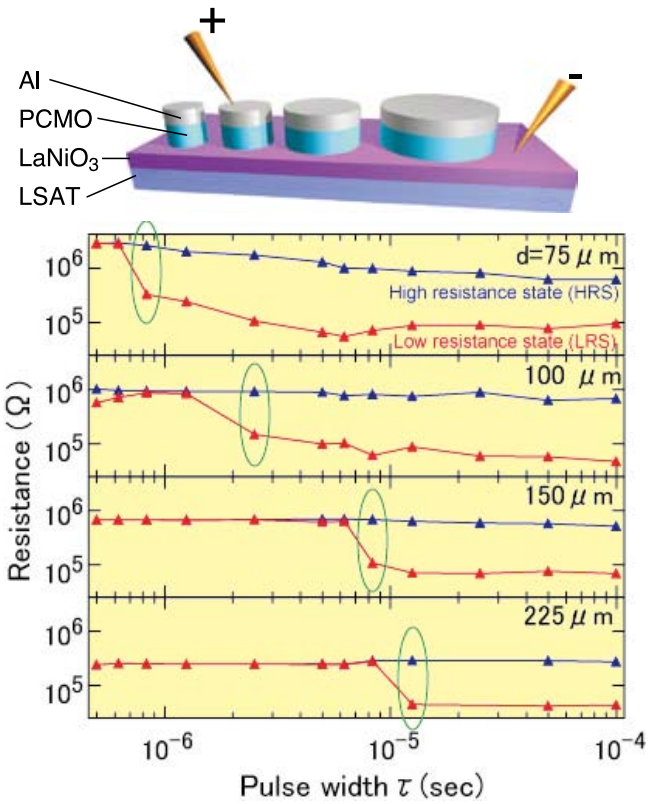

Fig. 1. Top: Structure of the resistance switching devices grown on $(LaAlO_3)_{0.3}$-$(Sr_2AlTaO_6)_{0.7}$ (LSAT) substrate. The bottom electrode is a metallic $LaNiO_3$ layer. Resistive switching occurs in the $Pr_{0.7}Ca_{0.3}MnO_3$ (PCMO) layer. As shown in the time-dependent switching characteristics, smaller devices can be switched faster by applying positive or negative voltage pulses to the top Al electrode.

for different device sizes. The static high or low resistance states can be obtained by applying short positive or negative 'write' pulses to the device. As shown by the switching data in Fig. 1, the switching time becomes smaller as the devices are scaled to smaller size, which means that when scaled to suitable small feature size, it may be possible to achieve ns-scale switching speeds.

Although a trap-controlled space-charge-limited current mechanism has been identified as the most likely candidate for explaining the resistance change, the precise reason why the effect only appears at a manganite-aluminum interface remains a subject of atomic-scale interface studies. It is as yet not clear how strong electric fields drive structural changes in oxide heterostructures. Future work within this collaboration aims to use the resistance switching effect as a tool for detecting field-driven structural changes in oxide nanostructures.

References

[1] A. Maniwa *et al.*, J. Magn. Magn. Mater. **310**, 2237 (2007)
[2] H. Wadati *et al.*, J. Magn. Magn. Mater. **310**, 963 (2007)
[3] K. Tsubouchi *et al.*., Adv. Mat. **19**, 1711 (2007)
[4] I. Ohkubo *et al.*, Mat. Sci. Eng. B **148**, 13 (2008)

Authors

I. Ohkubo[a], H. Kumigashira[a,e], A. Fujimori[b,c], M. Oshima[a], H. Wadati[b,c], A. Maniwa[a], K. Okano[a], K. Tsubouchi[a], Y. Matsumoto[d], K. Itaka[e,f], T. Ohnishi, T. Harada[a], M. Kawasaki[g], H. Koinuma[e,f,h], and M. Lippmaa
[a] Dept. of Applied Chemistry, University of Tokyo
[b] Dept. of Physics, University of Tokyo
[c] Dept. of Complexity Science and Engineering, University of Tokyo
[d] Materials and Structures Laboratory, Tokyo Institute of Technology
[e] CREST, Japan Science and Technology Corporation
[f] Graduate School of Frontier Sciences, University of Tokyo
[g] Institute for Materials Research, Tohoku University
[h] National Institute for Materials Science

Mechanical Spin Pumping in Superfluid ^{3}He A_1 phase

H. Kojima and H. Ishimoto

When liquid ^{3}He is cooled down to low enough temperatures in a magnetic field, the normal liquid first makes a transition into superfluid A_1 phase at T_{c1} and then into superfluid A_2 phase at a lower temperature T_{c2}. The most important aspect of the A_1 phase is that its superfluid component is totally spin-polarized along the magnetic field. It is a kind of ferromagnetic superfluid. A mass superflow is then simultaneously a spin flow. The phase transition into the A_1 phase is accompanied by the spontaneous breaking of relative spin-gauge symmetry. Interesting hydrodynamic effects occur in the A_1 phase such as a unique magnetic fountain pressure effect which was predicted by Liu [1] and established by Kojima [2]. Our recent experiments on this interesting magnetically driven superflow show a peculiar spin relaxation that is dependent on temperature and magnetic fields [3]. The results can be interpreted in terms of intrinsic spin relaxation based on Leggett and Takagi theory [4] and the predicted presence of small but increasing presence of minority spin pair condensate in A_1 phase [5].

In these measurements, we recognized a mechanical spin pumping and found a new method to derive the spin relaxation time in the A_1 phase. A sample cell has a large reservoir that is connected to a small detector chamber through a super leak made of three channels of width 18 μm. A flexible Myler membrane dividing the two chambers forms a capacitance with a fixed electrode. It works as a very sensitive differential pressure sensor and also as a pump to produce a polarized spin flow into the detector chamber. A pulsed large DC voltage (about 30 V) on the capacitance sensor induces a simultaneous mass and spin superfluid flow into the small chamber (spin pump). After thermal equilibrium, release of the DC voltage causes a sudden pressure drop. The sudden drop (ΔP) is a consequence of reversed superfluid flow through the superleak. It is compensated by the produced spin density difference Δ S). In the A_2 phase, ΔP suddenly returns to zero, whereas in the A_1 phase there still remains a slow relaxation (Fig. 1). This slow relaxation is due to spin relaxation that is peculiar to A_1 phase. The spin relaxation times derived from the slow decay times are in good agreement with those obtained in the magnetic fountain effect. This fact supports our

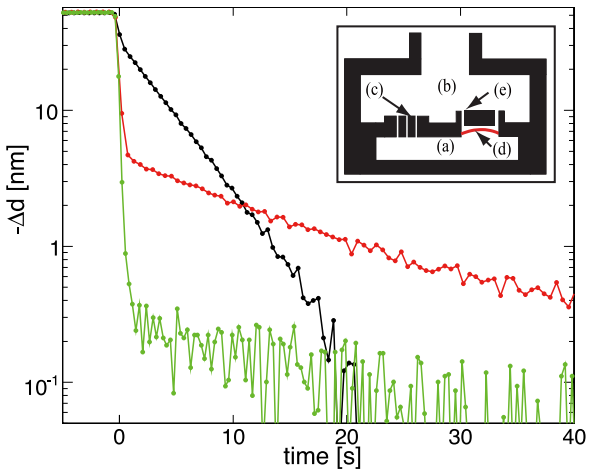

Fig. 1. Membrane' s displacement corresponding to the voltage change in the A_1 , A_2 and normal phase at 21 bars and 8T. (A_1: red, A_2: green, normal: black)

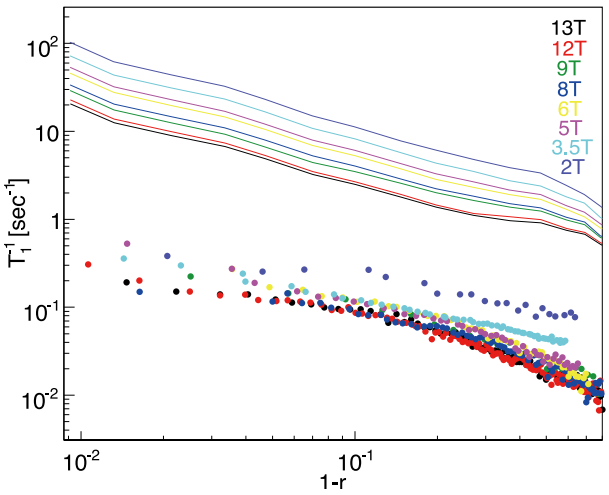

Fig. 2. The spin relaxation rate derived from mechanical effects at 21 bars and various magnetic fields as a function of reduced temperature.

interpretation that the observed slow relaxation stems from spin relaxation. After a simple analysis, a device independent intrinsic spin relaxation rate is obtained as shown in Fig. 2. The temperature dependence agrees pretty well with the above theoretical estimation, although the amount of the minority spin condensate seems to be smaller than predicted.

References
[1] M. Liu, Phys. Rev. Lett. **43**,1740 (1979).
[2] R. Ruel and H.Kojima, Phys. Rev. B **28**,6582 (1983).
[3] A. Yamaguchi, S. Kobayashi, H. Ishimoto, and H. Kojima, Nature **444**, 909 (2006).
[4] A. J. Leggett and S.Takagi, Annals of Physics **106**, 79 (1977).
[5] H. Monien and L. Tewordt, J. Low Temp. Phys. **60**, 323 (1985).

Authors
A. Yamaguchi, K. Suzuku, Y. Aoki, H. Ishimoto, and H. Kojima[a]
[a]Serin Physics laboratory, Rutgers University

Discovery of Coherent Precession of Magnetization in Superfluid ^{3}He-A-phase*

Yu. M. Bunkov, T. Mizusaki, and M. Kubota

We report the first observation of coherent quantum precession (**CQP**) of magnetization in superfluid ^{3}He-A in aerogel [1]. The coher- ent precession in bulk ^{3}He A-phase is un-stable due to the positive feedback of spin supercurrent to the gradient of phase of pre- cession. It was predicted that the homogene-ous precession will be stable if the orbital momentum of ^{3}He-A could be oriented along the magnetic field [2]. We have succeeded to prepare this configuration by emerging ^{3}He in uniaxially deformed anisotropic aerogel [3].

Superfluid ^{3}He is a unique superfluid composed of p type Cooper pairs. Because of large internal freedom of the Cooper pairs, there are multiple superfluid phases and so on. The superfluid wave function can be expressed as a product of mass, orbital momentum and magnetization (spin) components. The coherent precession of magnetization was observed early in superfluid ^{3}He-B [4]. Due to the concave shape of dipole-dipole interaction and negative feed-back of spin supercurrent (the quantum flow of magnetization due to the gradient of the phase of

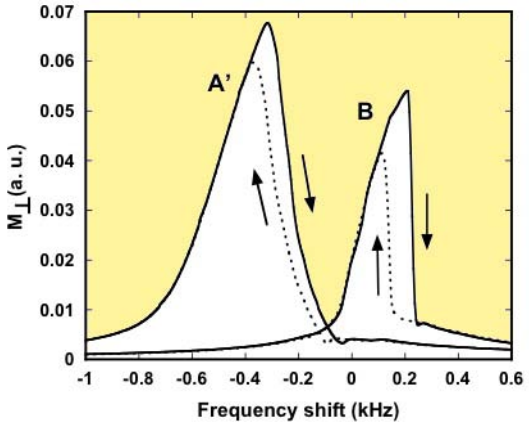

Fig. 1. Formation of the coherent precession of magnetization; the CQP in A-like phase at $0.8T_{ca}$ (labeled by A') and the HPD in B phase at $0.7T_{ca}$ (labeled by B). The solid curves are taken at an rf-field (3volts) for upward sweep and the dotted one for downward sweep. The relative positions to Larmor fre- quency(marked as 0) are just as expected.

spin part of order parameter), the coherent precession of magnetization in ^{3}He-B arises spontaneously even in inhomogeneous magne-tic field, as was discovered in1984 by Borovik- Romanov *et al.* [4]. This effect was named a Ho-mogeneously Precessing Domain (**HPD**), due to the splitting of the magnetization in the cell into two domains, stationary one and the other with the coherent precession of magnetization deflected by the angle slightly above the magic angle of 104°. Recently the **HPD** was identified as magnon Bose-Einstein condensation by Bunkov and Volovik [5]. Here we report the first observation of the Coherent Quantum Precession (**CQP**) of magnetization in A-like Phase in uniaxially deformed aerogel, where the ***l***-vector in the orbital part of the order parameter is oriented along the magnetic field [3,6]. We call the coherent precession in A-phase as the **CQP**, distinguishing it from the **HPD** in B-phase. **CQP** has been searched for for a long period of time, but in bulk A phase ***l***-vector tends to be perpendicular to magnetic field ***H***. **CQP** can appear only under a special condition when ***l***-vector is forced to be in parallel with ***H***. This has been realized in ^{3}He-A (see Fig.1, 2) immersed in a uni-axially deformed aerogel [3]. A basic difference in the observation is that in **CQP** the entire magnetization precesses uniformly with a tipping angle β determined by frequency sweep Δf from cw NMR, while the **HPD** precession occurs in a domain with $\beta > 104°$.

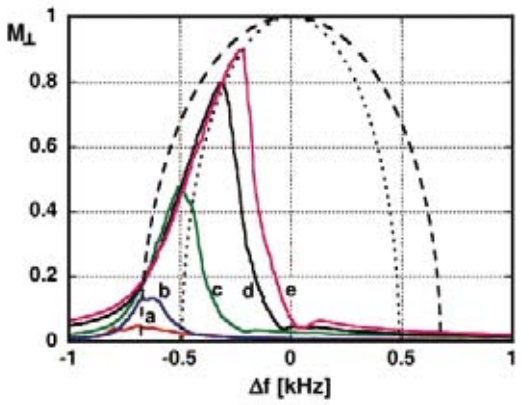

Fig. 2. The normalized amplitude of NMR signal by $M\perp(\beta=90°)$ while sweeping frequency upward at dif- ferent excitations v_{rf} (a: 0.1V, b: 0.5V, c: 1.5V, d: 3V, e: 4V). The dashed line corresponds to the theoretical dependence of $M\perp$ on the tipping angle dependent frequency shift given by $\Delta\omega = -(\Omega^2_A/2\omega L)\cos\beta$ with the maximum frequency shift chosen at the peak of signal a and the dotted line corresponds to that for the maximum frequency shift chosen at the right edge of signal a. See details in [1].

∗ Prof. Yuryi Bunkov has been selected for a Fritz London Prize winner 2008, together with the coauthors of reference[4] and the present work is an extension of their original finding in superfluid ^{3}He B phase in 1984 into superfluid ^{3}He A phase, which has been searched for ever since that time.

References

[1] T. Sato *et al.*, arXiv:0804.2994, and submitted to PRL.
[2] Yu. M. Bunkov and G. E. Volovik, Europhys. Lett. **21**, (8) 837 (1993).
[3] T. Kunimatsu *et al.*,JETP Lett. **86**, 216 (2007).
[4] A. S. Borovik-Romanov, Yu. M. Bunkov, V. V. Dmitriev, and Yu. M. Mukharskiy, JETP Lett. **40**, 1033 (1984); I. A.Fomin, JETP Lett. **40**, 1036 (1984).
[5] Yu. M. Bunkov and G. E. Volovik, Phys. Rev. Lett. **98**, 265302 (2007).
[6] T. Kunimatsu *et al.*, J. Low Temp. Phys. **150**, 435 (2008).

Authors

T. Sato, T. Kunimatsu[a], K. Izumina, A. Matsubara[a,b] O. Ishikawa[c], Y. Sasaki[b], M. Kubota, T. Mizusaki[a,b], and Yu. M. Bunkov[d]
[a]Department of Physics, GraduateSchool of Science, Kyoto University
[b]Research Center for Low Temperature and Materials Sciences, Kyoto University
[c]Department of Physics, GraduateSchool of Science, Osaka City University
[d]MCBT, Institut N´eel, CNRS/UJF

Pressure Effect on the Electronic State in $CeTl_3$

T. Endo, R. Settai, and Y. Uwatoko

When pressure is applied to cerium-based magnetic compounds, various interesting phenomena such as non-Fermi liquid behavior, heavy fermion state and pressure-induced superconductivity appear in the vicinity of the quantum critical point where the Néel temperature T_N is suppressed to zero. $CeTl_3$ is an antiferromagnet with

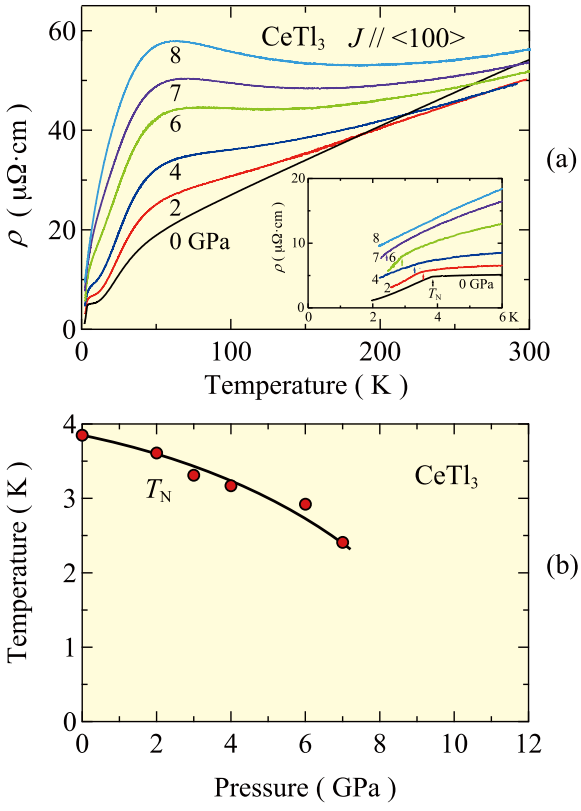

Fig. 1. (a) Temperature dependence of the electrical resistivity under pressure in $CeTl_3$ and (b) Pressure phase diagram of the Néel temperature T_N in $CeTl_3$.

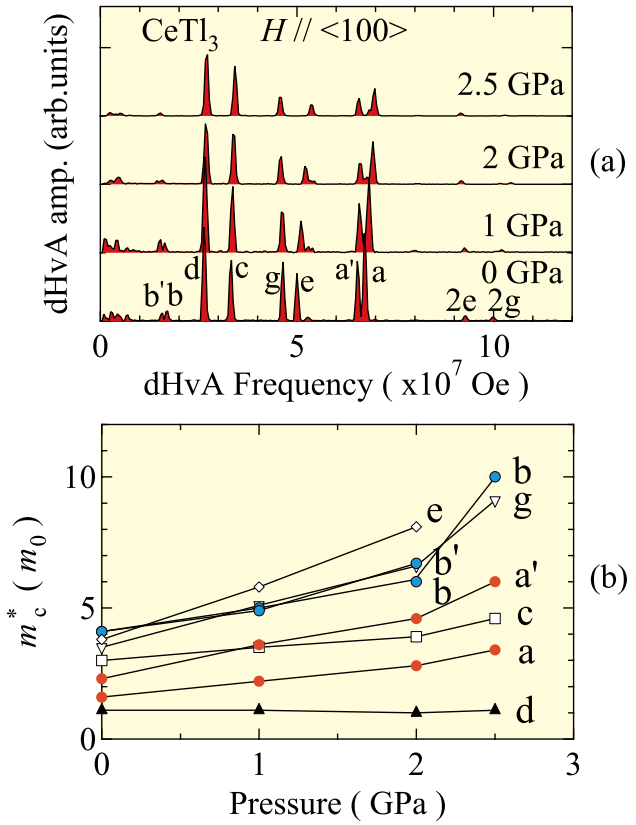

Fig. 2. (a) FFT spectra under pressure and (b) pressure dependence of the cyclotron effective massin $CeTl_3$

T_N = 3.9K [1]. $CeTl_3$ is a good reference compound for an antiferromagnet $CeIn_3$, which exhibits the pressure-induced superconductivity at 0.2 K around the critical pressure P_c = 2.5 GPa [2]. We studied the electrical resistivity under pressure in $CeTl_3$ using a cubic anvil cell up to 8 GPa.

Figure 1(a) shows the temperature dependence of the electrical resistivity under several pressures in $CeTl_3$. A shoulder-like resistivity peak around 50 K, which is due to the combined phenomenon between the crystalline electric field and Kondo effects, is enhanced with increasing pressure. The electrical resistivity at 8GPa is typical for heavy fermion compounds such as $CeCu_6$. Néel temperature T_N, which is indicated by an arrow, is found to decrease with increasing pressure, ranging from T_N = 3.9 K at ambient pressure to 2.4 K at 6GPa. The antiferromagnetic ordering was not observed at 8GPa because the measurement was carried out down to about 2 K. We plotted the Néel temperature as a function of pressure in Fig. 1(b). The critical pressure P_c was not well defined in the present experiment, but most likely estimated to be about 10GPa.

In order to investigate the change of the electronic state under pressure in $CeTl_3$, we measured the de Haas-van Alphen (dHvA) effect under pressure. Figure 2 shows (a) the fast Fourier transformation (FFT) spectra under pressure and (b) the pressure dependence of the cyclotron effective mass of the dHvA branches. The observed dHvA branches are similar to those of $LaIn_3$. This result indicates that the 4*f*-electron in $CeTl_3$ is localized.The dHvA frequenciesare almost unchanged under pressure. On the other hand, the cyclotron masses increase with increasing pressure. The increase of the cyclotron mass reflects the approach to the quantum critical point by applying pressure. Further study below 2 K at around 10 GPa is necessary to investigate the quantum critical behavior such as pressure-induced superconductivity.

References

[1] R. A. Elenbaas *et al.*, J. Magn. Magn. Mater. **15-18**, 1218 (1980).
[2] N. D. Mathur *et al.*, Nature **394**, 39 (1998).
[3] I. Umehara *et al.*, J. Phys. Soc. Jpn. **60**, 591 (1991).

Authors

T. Endo[a], M. Nakashima[b], R. Settai[a], D. Aoki[c], Y. Ōnuki[a], and Y. Uwatoko
[a]Graduate School of Science, Osaka University
[b]Department of Physics, Faculty of Science, Shinsu University
[c]DRFMC/SPSMS, CEA-Grenoble, France

Motional Behavior of Fluorobenzene Guests Imprisoned in a Hofmann-dahxn Clathrate 1D Cavity

A. Nagahara, S. Nishikiori, and O. Yamamuro

The state of a system in which molecules are interacting with each other has been an important research target in various viewpoints. Many variations and situations are considered for such systems and many cases have been widely investigated. We here examined a simple case as following. Polar molecules are arrayed one-dimensionally. The molecules can undergo not translational motion but reorientational motion (Fig. 1). Simply saying, this situation is similar to 1D Ising model made with macro species.

To realize the above system we used a clathrate compound. Clathrate compounds are formed with a host and guests. The host is a kind of cage and the guests are imprisoned in the host. Depending on clathrate hosts there are many structural variations. We choose the Hofmann-dahxn type clathrate [1] including fluorobenzene (FBz) as guests, $Cd(dahxn)Ni(CN)_4$·FBz. The host of the clathrate is a metal complex of $Cd(dahxn)Ni(CN)_4$ which has a 3D framework structure made with octahedral Cd(II), square planar Ni(II) and bidentate CN^- and 1,6-diaminohexane (dahxn).

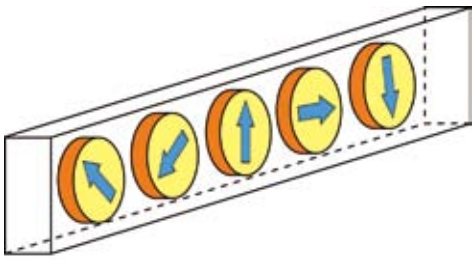

Fig. 1. 1D array of polar molecules which are allowed to perform not translational but reorientational motion.

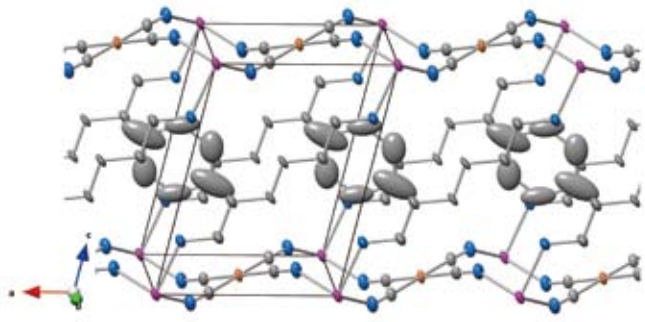

Fig. 2. Crystal structure of $Cd(dahxn)Ni(CN)_4$·FBz at 153K. Crystal data: $C_{16}H_{21}N_6FCdNi$, monoclinic, $P2/m$, a = 7.0894(3)Å, b = 7.5993(3)Å, c = 9.3698(7) Å, β = 103.144(2)°, Z = 1. All FBz guests are on the plane of y =1/2. The orientation of each FBz guest is distributed to two inverted directions. H atoms are omitted for clarity.

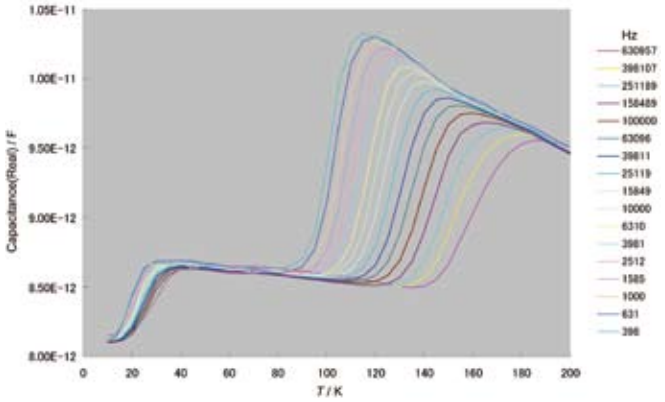

Fig. 3. Temperature dependence of dielectric permittivity for Cd(dahxn)Ni(CN)$_4$·FBz.

Figure 2 shows the crystal structure of the clathrate. In the 3D framework host a 1D channel-like cavity with a section of *ca.* 7.6 Å × *ca.* 9.2 Å running straightly along the *a* axis of the crystal is formed. In this channel-like cavity FBz guests, whose dipole moment is 1.63 D, are lined up along the *a* axis at regular intervals. The molecular planes of all guests in the cavity are on a plane which is parallel to the *ac* plane and is as y =1/2.

The single crystal X-ray diffraction experiments at 298 K and 153 K revealed that the orientation of the FBz guests is distributed to two inverted directions. ^{2}H-NMR powder patterns measured on the clathrate including deuterated FBz showed that the guests undergo reorientation between the two inverted orientations at least above 123 K. This motional mode is similar to that of the spin in Ising model.

To elucidate the motional behavior of the guests in lower temperature region dielectric permittivity was measured by using a homemade cryostat for dielectric measurements. Powdered sample was packed in a cylindrical cell and the measurement was carried out between 300 K and 6 K in temperature and between 10^{-1} Hz and 10^6 Hz in frequency. Figure 3 shows the real part of the capacitance observed. Two dielectric dispersions and no sign of phase transition can be found at once. The large dispersion ranging from 200 K to 70 K corresponds to the inversion motion observed in the ^{2}H-NMR spectra. If the orientation of the guests falls into an ordered state, a first order phase transition accompanied with a change of the crystal structure must take place. However, no such sign was observed. From 40 K to 10 K a small dispersion was observed. Appearance of dispersion suggests that molecular motion is thermally activated. The small dispersion indicates that the guests undergo thermal motion even at 10 K. This motion is considered to be a vibrational reorientation at the bottom of the potential surface for the inversion motion in the higher temperature region. The guests are hardly considered to climb over the potential wall and to form an ordered state at this low temperature. Perhaps, this disordered state is not dissolved and the system falls to a glassy state before reaching 0 K. Formation of a glassy state is not unusual for macro systems. However, such transition usually takes place in higher temperature region. No freezing even at *ca.* 10 K observed in our macro system is a rare case. Although this system is resemble to 1D Ising model, three-dimensional molecular interaction from surroundings actually exists more or less because our system is a real object. Perhaps, the structure of this clathrate host cancels or reduces the three-dimensional interaction to bring the unusual phenomenon observed here.

References

[1] T. Iwamoto, *Comprehensive Supramolecular Chemistry*, ed. J. L. Atwood, J. E. D. Davies, D. D. MacNicol, F. Vögtle, and J-M. Lehn (Pergamon, Oxford, 1996), vol. **6**, ch. 19, pp 643-690; T. Iwamoto, J. Inclu. Phenom. **24**, 61 (1996).

Authors

A. Nagahara[a], S. Nishikiori[a], and O. Yamamuro

[a]Department of Basic Science, Graduate School of Arts and Sciences, The University of Tokyo

TEM Study of the Two-Dimensional Quantum Antiferromagnets (CuCl)LaNb$_2$O$_7$ and (CuBr)Sr$_2$Nb$_3$O$_{10}$

H. Kageyama, M. Ichihara, and Y. Ueda

Chimie douce, solid-state reactions at relatively low temperatures, *i.e.*, away from thermodynamic equilibrium offer rational design of the magnetic lattices in nonmolecular solids. Recently, various exotic quantum magnetic phenomena have emerged from a new class of S = 1/2 layered transition-metal oxyhalides (CuX)[$A_{n-1}B_n$O$_{3n+1}$] (where X = Cl$^-$, Br$^-$, A = La^{3+}, Ca^{2+}, Na$^+$···, B = Nb^{5+}, Ta^{5+}, Ti^{4+}···, n = 2, 3), obtained by low-temperature ion-exchange reactions [1]. They range from collective singlet-ground states in (CuCl)LaNb$_2$O$_7$ (Fig. 1(a)) [2-4], a collinear order at 32 K with a reduced magnetic moment in (CuBr)LaNb$_2$O$_7$ [5], to successive phase transitions and 1/3 magnetization plateaus in (CuBr)Sr$_2$Nb$_3$O$_{10}$ (Fig. 1(b)) [6], which may be mapped onto the so-called J_1-J_2 model.

In order to obtain universal understanding of the magnetism in this series of materials, precise structural analysis is required. Considering that single crystals are not in our hands (since they are metastable compounds and hence could not be grown by high temperature melting method), transmission electron microscopy (TEM) will offer crucial information on the space group, as well as possible superstructures. The TEM experiments were carried out typically at room temperature using a JEM2010F system with an operating voltage of 200 kV. The specimen was finely ground in methanol and then placed on a Cu microgrid mesh for TEM observation

Shown in Fig. 2(a) is the [001] zone lattice image of (CuCl)LaNb$_2$O$_7$ [7] that demonstrates contrast with a special

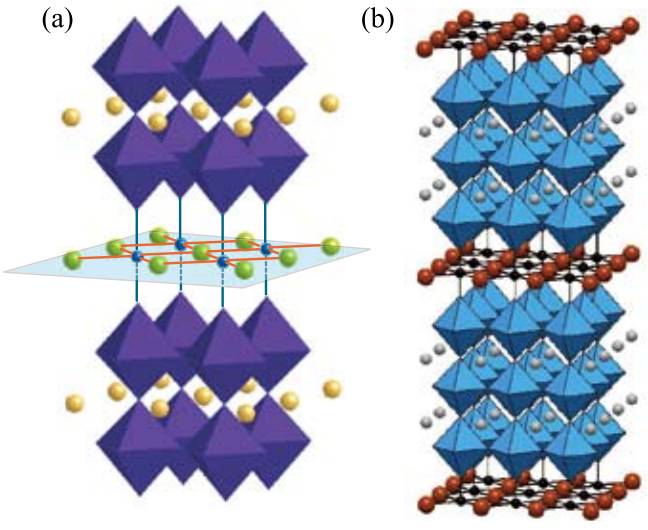

Fig. 1. Crystal structure of (a) (CuCl)LaNb$_2$O$_7$ and (b) (CuBr)Sr$_2$Nb$_3$O$_{10}$, where the CuCl and CuBr layers providing the S = 1/2 square lattice are magnetically separated by the non-magnetic perovskite slab of n = 2 LaNb$_2$O$_7$ and n = 3 Sr$_2$Nb$_3$O$_{10}$, respectively.

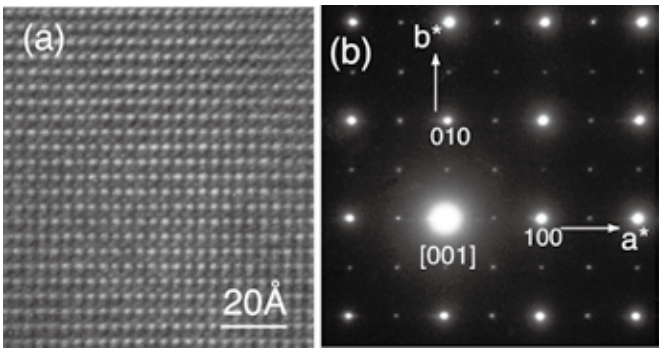

Fig. 2. High-resolution transmission electron microscopy image of (CuCl)$LaNb_2O_7$ at room temperature, obtained along the [001]-zone axis and the corresponding electron diffraction pattern, where indices are given based on the primitive unit cell for the double-layered perovskite.

period of about 0.4 nm along <100>, consistent with the lattice parameter. However, the corresponding electron diffraction (Fig. 2(b)) has revealed weak reflections such as (1/2, 0, 0) or (0, 1/2, 0), in addition to strong fundamental reflections relevant to the reported crystal structure. The weak reflections are commensurate and indicate the doubling of the lattice period of both *a*- and *b*-axes, *i.e.*, the size of the unit cell is given by $2a \times 2b$. Such a superstructure has not been detected even by high-Q resolution synchrotron X-ray diffraction, presumably due to tiny modulation of the atoms and/or small domain size. A similar superstructure has been recently obtained by the TEM study of (CuBr)$Sr_2Nb_3O_{10}$ [8]. It is considered that the superstructure formation, which give a deviation of the simple J_1-J_2 model, plays crucial role in the spin-singlet state in (CuCl)$LaNb_2O_7$ and the 1/3 magnetization plateau in (CuBr)$Sr_2Nb_3O_{10}$ is still not clear.

References

[1] 陰山洋, 北野太郎, 大場紀章, 網代芳民, 吉村一良, 西正和, 廣田和馬, 鳴海康雄, 金道浩一, 萩原政幸, 固体物理 **41**, 129 (2006).
[2] H. Kageyama, T. Kitano, N. Oba, M. Nishi, K. Hirota, L. Viciu, J. B. Wiley, J. Yasuda, Y. Ajiro, and K. Yoshimura, J. Phys. Soc. Jpn. **74**, 1702 (2005).
[3] H. Kageyama, J. Yasuda, T. Kitano, K. Totsuka, Y. Narumi, M. Hagiwara, K. Kindo, Y. Baba, N. Oba, Y. Ajiro, and K. Yoshimura, J. Phys. Soc. Jpn. **74**, 3155 (2005).
[4] A. Kitada, Z. Hiroi, Y. Tsujimoto, T. Kitano, H. Kageyama, Y. Ajiro, and K. Yoshimura, J. Phys. Soc. Jpn. **76**, 093706 (2007).
[5] N. Oba, H. Kageyama, T. Kitano, J. Yasuda, Y. Baba, M. Nishi, K. Hirota, Y. Narumi, M. Hagiwara, K. Kindo, T. Saito, Y. Ajiro, and K. Yoshimura, J. Phys. Soc. Jpn. **75**, 113601 (2006).
[6] Y. Tsujimoto, Y. Baba, N. Oba, H. Kageyama, T. Fukui, Y. Narumi, K. Kindo, T. Saito, M. Takano, Y. Ajiro, and K. Yoshimura, J. Phys. Soc. Jpn. **76**, 063711 (2007).
[7] M. Yoshida, N. Ogata, M. Takigawa, J. Yamaura, M. Ichihara, T. Kitano, and H. Kageyama, J. Phys. Soc. Jpn. **76**, 104703 (2007).
[8] Y. Tsujimoto, Y. Baba, T. Watanabe, A. Kitada, H. Kageyama, Y. Ajiro, K. Yoshimura, M. Ichihara, and Y. Ueda, submitted to Solid State Science.

Authors

H. Kageyama[a], Y. Ajiro[a], K. Yoshimura[a], M. Ichihara, and Y. Ueda
[a]Kyoto University

Single Crystal Growth of a New Pyrochlore Frustrated Magnet $Pr_2Zr_2O_7$ by the Floating Zone Method

K. Matsuhira and Z. Hiroi

Geometrical frustration can lead to novel phenomena such as a macroscopic degeneracy in the ground state and a spin freezing with no long-ranged ordering (LRO). Pyrochlore compounds have been attracting a great deal of interest because spins reside on the vertices of corner-shared tetrahedra (Fig.1). A strong frustration effect is expected in the pyrochlore magnets.

Recentry, we revealed that the pyrochlore oxide $Pr_2Zr_2O_7$ is a local <111> Ising pyrochlore antiferromagnet (Curie-Weiss temperature $\Theta_{CW}=-0.55$ K). The magnetism of $Pr_2Zr_2O_7$ arises from Pr^{3+} ($4f^2$, J=4) ions, as Zr^{4+} ($4d^0$) is non-magnetic. The polycrystalline sample does not exhibit any LRO at least down to 76 mK. Instead, a spin freezing behavior is observed below 0.3 K [1]. The crystal electric field ground state is non-Kramers doublet with a local <111> Ising magnetic anisotropy. Theoretically, the antiferromagnetic ground state of a single tetrahedron of spins with a local <111> Ising magnetic anisotropy consists of alternate tetrahedra with 4 spins in or 4 spins out (Fig. 1) [2]. However, LRO with 4 spins in or 4 spins out have not yet been reported in the pyrochlore magnets so far. The local <111> Ising pyrochlore antiferromagnet is firstly reported in $Tb_2Ti_2O_7$ [3]. $Tb_2Ti_2O_7$ remains in a fluctuating paramagnetic spin-liquid state down to 70 mK. Why does not the <111> Ising pyrochlore antiferromagnet indicate LRO? This question is a fundamental problem in the frustrated magnetism.

We consider that $Pr_2Zr_2O_7$ is a key compound to solve the problem. We need a good single crystal of $Pr_2Zr_2O_7$ to perform various measurements. Single crystal growth of Zr pyrochlore oxides has not been reported so far. We have performed the single crystal growth of pyrochlore titanates ($Ln_2Ti_2O_7$: Ln=Gd, Tb, Dy, Ho) by the floating-zone method using an infrared furnace equipped with four halogen lamps (4×1.5kW) and elliptical mirrors so far. However, we could not form a melt zone in the same way because the melting point of $Pr_2Zr_2O_7$ is higher. Next, we tried to use an infrared furnace equipped with four Xenon lamps (4×3kW) and elliptical mirrors. We encountered some difficulties due to

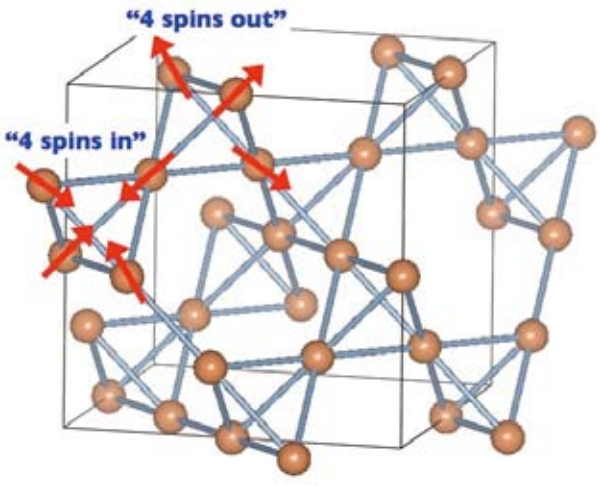

Fig. 1. Pyrochlore lattice: In Pyrochlore oxides $A_2B_2O_7$, both A and B sites form the corner-shared tetrahedral network. Antiferromagnetic ground states (4 spins in or 4 spins out) of a single tetrahedron of spins with a local <111> Ising magnetic anisotropy are shown.

Fig. 2. Single crystal of pyrochlore oxide $Pr_2Zr_2O_7$.

the high melting point. The biggest problem was the lack of Pr site in the single crystal due to the evaporation of Pr_2O_3. In order to avoid the lack of Pr site, we prepared the Pr-enriched samples in the starting composition.

We have succeeded for the first time in growing a good single crystal of $Pr_2Zr_2O_7$ after much trial and error. The crystal is shown in Fig. 2. The crystal was grown under O_2 gas flow to avoid oxygen deficiency. The growth rate was 4.5 mm/h. The powder XRD pattern shows the pyrochlore phase. The SEM-EDS analysis indicated that the ratio of Pr/Zr is 1.00 in the top part of the single crystal. Therefore, the good quality of this crystal was confirmed. Various measurements to clarify the magnetic properties are currently in progress.

References

[1] K. Matsuhira, C. Sekine, C. Paulsen, M. Wakeshima, and Y. Hinatsu, Physical Society of Japan 2007 Spring Meeting (20aTB-8).

[2] S. T. Bramwell and M. J. Harris, J. Phys.: Condens. Matter **10**, L215 (1998).

[3] J. S. Gardener, S. R. Dunsiger, B. D. Gaulin, M. J. P. Gingras, J. E. Greedan, R. F. Kiefl, M. D. Lumsden, W. A. MacFarlane, N. P. Raju, J. E. Sonier, I. Swainson, and Z. Tun, Phys. Rev. Lett. **82**, 1012 (1999).

Authors

K. Matsuhira[a], Z. Hiroi, T. Kitazawa, Y. Kiuchi, S. Takagi [a]

[a]Kyushu Institute of Technology

First-Principles Study of Multiferroic Oxides

T. Oguchi, T. Shishidou, and Y. Uratani

Materials which have more than one ferro orders are originally called “multiferroics” and may be possibly applied not only to multi-value devices but also to novel response phenomena originating from the cross correlation between different ferro orders. For example, the magnetic response to an electric field and the electric response to an magnetic field are known as magneto-electric or electro-magnetic effect, and a cross correlation between the electric polarization and the lattice distortion is as piezoelectric effect. Nowadays, materials with a cross correlation between different order parameters are generally called multiferroics. Here we report first-principles studies of the multiferroic oxides consisting of ferro (or antiferro) magnetism and ferroelectricity simultaneously. Several perovskite-type oxides are well known as typical multiferroics. By investigating the electronic structure of the multiferroic and related materials and by elucidating the microscopic mechanisms of multiferro orders, new candidate materials are proposed.

$BiMnO_3$ is among the best known ferromagnetic and ferroelectric multiferroic materials. The centrosymmetric orthorhombic structure *Pbnm* at high temperature undergoes a phase transition to a non-centrosymmetric monoclinic one $C2$ around 750-770K and a magnetic transition from the paramagnetic to ferromagnetic phase at about 100K. The multiferroic monoclinic crystal determined by a neutron diffraction measurement can be seen as extremely deformed perovskite structure. A first-principles calculation for monoclinic $BiMnO_3$ [1] shows that the dy orbital extended along the Mn-O bond elongated by the Jahn-Teller effect is only occupied, forming antiferro orbital order as shown in Fig. 1, and that the ferromagnetic state is more stable than the antiferromagnetic. It is found based on a frozen-phonon calculation that the covalent bond due to hybridization between the Bi-p and O-p orbitals results in off-centering instability. However, two kinds of Bi show almost opposite displacement to each other and the resultant electric polarization turns out to be quite small ($<0.01 C/m^2$).

$PbVO_3$ and $BiCoO_3$ were synthesized experimentally by the high-pressure technique and show large tetragonal distortion and off-centering displacements. The main issue here is how the energy gaps are formed for the d^1 (d^6) configuration in V^{4+} (Co^{3+}) in relation to the large tetragonal distortion. It is found in a first-principles calculation [2] that the tetragonal distortion together with the observed off-centering displacement introduces the opposite crystal-field splitting, lower xy and higher (yz, zx), to realize an insulating electronic structure. In addition, an antiferromagnetic coupling may take place between the neighboring xy states via O-$p\pi$ on the ab plane, resulting in stable C-type or G-type antiferromagnetic order. The stability of the C-type or G-type antiferromagnetic order has been confirmed by the total-energy results calculated for different magnetic structures. Two instability modes to off-centering displacements are obtained by frozen-phonon calculations for the tetragonal centrosymmetric structure. One is the mode in which the transition-metal ion moves in the opposite

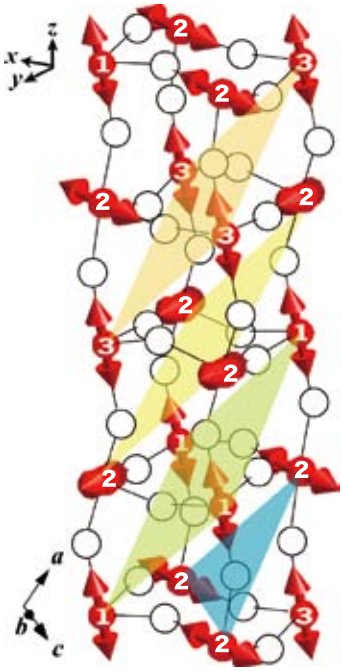

Fig. 1. Schematic view of the orbital ordering of Mn-d in $BiMnO_3$. Arrows indicate the occupied dy orbital directions at the Mn sites, of which three kinds are denoted by 1, 2 and 3. Open circles denote the O sites.

direction to the O octahedron and the other is that Pb or Bi ion is displaced against the octahedron including the transition-metal ion. Actual stable structure observed can be regarded as a superimposed one of these two instability modes. From the Berry-phase calculations, the electric polarization is predicted to be 1.52C/m^2 for $PbVO_3$ and 1.79C/m^2 for $BiCoO_3$.

On the basis of the knowledge deduced from the first-principles calculations stated above, new multiferroic oxides with ferromagnetism and ferroelectricity have been designed [3]. The target materials are chosen to be double-perovskite oxides with Bi at the *A* site, $Bi_2BB'O_6$, where *B* and *B'* are transition-metal ions with the finite number of *d* electrons. In the double-perovskite structure, two kinds of the transition-metal ions are located in a NaCl-type manner, where the neighboring *B* and *B'* ions form 180° structure via O ion. The super-exchange coupling between the neighboring *B* and *B'* is ferromagnetic only for d^3-d^5 and d^3-d^8 combinations, according to the Goodenough-Kanamori rule. The cases satisfying both conditions are Cr^{3+}-Fe^{3+} and V^{2+}-Co^{4+} for d^3-d^5, and Mn^{4+}-Ni^{2+} and Cr^{3+}-Cu^{3+} for d^3-d^8. First-principles calculations for the cubic double-perovskite oxides with these combinations predict that, in Bi_2MnNiO_6, a stable ferromagnetic solution with d^3 and d^8 configurations is realized with zero-gap electronic structure and finite energy gaps may be expected by further lattice distortion due to ferroelectric instability. An experimental exploration of new double-perovskite multiferroic oxides has been made independently by using the high-temperature technique and has found that Bi_2MnNiO_6 is multiferroic [4]. A first-principles calculation for the observed monoclinic structure shows that the ferromagnetic state is more stable than the ferrimagnetic one and the electric polarization is found to be 0.28C/m^2.

References

[1] T. Shishidou, N. Mikamo, Y. Uratani, F. Ishii, and T. Oguchi, J. Phys.: Condens. Matter **16**, S5677 (2004).
[2] Y. Uratani, T. Shishidou, F. Ishii, and T. Oguchi, Jpn. J. Appl. Phys. **44**, 7130 (2005).
[3] Y. Uratani, T. Shishidou, F. Ishii, and T. Oguchi, Physica B **383**, 9 (2006).
[4] M. Azuma, K. Takata, T. Saito, S. Ishiwata, Y. Shimakawa, and M. Takano, J. Am. Chem. Soc. **127**, 8889 (2005).

Authors

T. Oguchi[a], T. shishidou[a], Y. Uratani[a], and F. Ishii[b]
[a]Hiroshima University
[b]Kanazawa University

Megagauss Spectroscopy of Single-Walled Carbon Nanotubes

H. Yokoi, E. Kojima, and S. Takeyama

Optical properties of single-walled carbon nanotubes (SWNTs) are governed largely by excitonic states because the exciton exists stably even at room temperature due to the one-dimensionality of their structures. It has been predicted theoretically that the excitonic state is split into singlet and triplet states due to valley mixing and exchange at K and K' points of the Brillouin zone because the electronic states are degenerate at the points. Among these excitonic states, only the gerade state of the singlet states is optically active ("bright") and the others are optically inactive ("dark"). It has been one of the most important problems in the properties of SWNTs which state locates

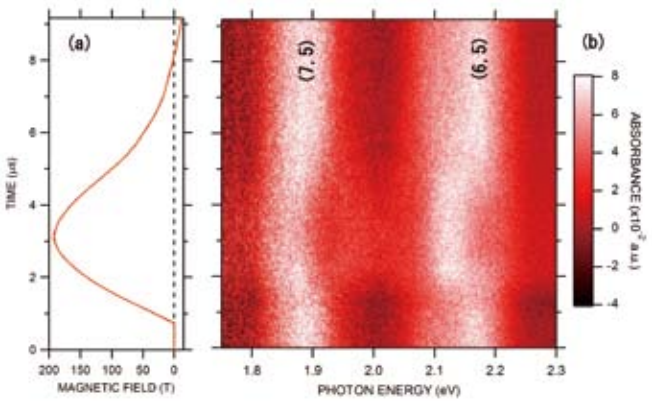

Fig. 1. Megagauss spectroscopy of excitonic states in single-walled carbon nanotubes (SWNTs) in a pulsed magnetic field. (a) Waveform of the megagauss field applied in parallel to the alignment of SWNTs. (b) Contour map of absorbance in an aligned SWNT film as a function of time and photon energy. The baseline of absorbance spectra has been removed. Each absorption peak is labeled by SWNT chirality index (*n,m*). The absorption peak for (7,5) SWNTs shifts toward the *lower* energy side, decreasing its intensity slightly, and a new peak emerges on the *higher* energy side while that for (6,5) SWNTs shifts toward the *higher* energy side, losing its intensity, and a new peak appears on the *lower* energy side with increasing magnetic field. The sample was at room temperature.

energetically lower between the singlet "bright" and "dark" excitonic states.

In order to approach this subject, we have conducted magneto-absorption measurements of aligned SWNT films in the visible light region at room temperature under ultra-short pulsed magnetic fields to 200 T using a single-turn coil system. We have succeeded to observe changing of absorption peaks originated from the second sub-band exciton in semiconducting SWNTs very clearly with increasing magnetic field in parallel to the alignment of SWNTs (Fig. 1). The following changes are recognized for SWNTs with a chiral vector of (6, 5) or (7, 5): The absorption peak observed at 0 tesla shifts toward the *higher* energy side and a new one appears on the *lower* energy side for the (6, 5) SWNT while the former shifts toward the *lower* energy side and the latter appears on the *higher* energy side for the (7, 5) SWNT. No modification of absorption spectra has been detected by the application of magnetic fields perpendicular to the alignment of SWNTs up to 200 T, which suggests that the spectral changes mentioned above are attributed to the Aharonov-Bohm effect.

These experimental results prove that it is the "dark" excitonic state in (6, 5) SWNT and the "bright" one in (7, 5) SWNT that situates at the lower energy side in the case of the singlet splitting of the second sub-band excitonic state. This configuration is different from that reported in the other magneto-luminescence studies where the "dark" one situates at lower energies in all of the investigated SWNTs. Further studies are required to resolve this contradiction.

Authors

H. Yokoi[a], E. Kojima, S. Takeyama, and N. Minami[b]
[a]Kumamoto University
[b]National Institute of Advanced Industrial Science and Technology

Non-magnetic Ground State and Excitation Gap in New Kagomé Antiferromagnet $Rb_2Cu_3SnF_{12}$

K. Morita, H. Tanaka, and K. Kindo

Two-dimensional S = 1/2 kagomé antiferromagnet (KAF) is one of the most attractive spin system from the viewpoint of synergy effect of quantum fluctuation and geometrical frustration. Although many theoretical and experimental studies have been carried out over few decades, the basic questions such as the ground state properties or the existence of the finite energy gap above the ground state are still open. Numerical studies [1,2] reveal that the energy spectrum of S = 1/2 KAF has the small gap between the singlet (non-magnetic) ground state to the lowest triplet (magnetic) state, and that the continuum of the non-magnetic excitations occupies up to the lowest triplet state. The experimental studies to test such a unique energy spectrum for S = 1/2 KAF have not been carried out yet due to the lack of suitable model substance [3,4].

Our recent studies on the new hexagonal antiferromagnet $Rb_2Cu_3SnF_{12}$[5] revealed that this compound has the slightly deformed kagomé layer with a $2a \times 2a$ enlarged cell as compared with the proper kagomé layer. Due to this crystal structure, there exist four kinds of the nearest-neighbor exchange interaction $J_1 \sim J_4$ between Cu^{2+}-ions, as depicted in the inset of Fig. 1. Temperature variation of the magnetic susceptibility shows the steep decrease below T < 70 K with lowering temperature, which is indicative of the existence of the energy gap between the non-magnetic ground state and the magnetic excited state. Using the exact diagonalization method with J_1/k_B = 234 K, J_2/k_B = 211 K, J_3/k_B = 187 K and J_4/k_B = 108 K, we have succeeded in reproducing the temperature variation of the magnetic susceptibility except for the low temperature region. To evaluate the excitation gap directly, we have performed the magnetization measurement, using pulsed high magnetic field. The magnetization curves for both field directions, $H||c$ and $H \perp c$, exhibit the bend anomaly at the field indicated by the arrows H_c in Fig 4. The energy levels of ground state and excited triplet state cross at H_c. The discrepancy of H_c for $H||c$ (~13T) and $H \perp c$ (~20T) is caused by the fact that the weak magnetic moment is induced by the field for $H \perp c$ even at the small field (see ref. [5]). This result shows the first evidence of the non-magnetic ground state in S=1/2 kagomé antiferromagnet.

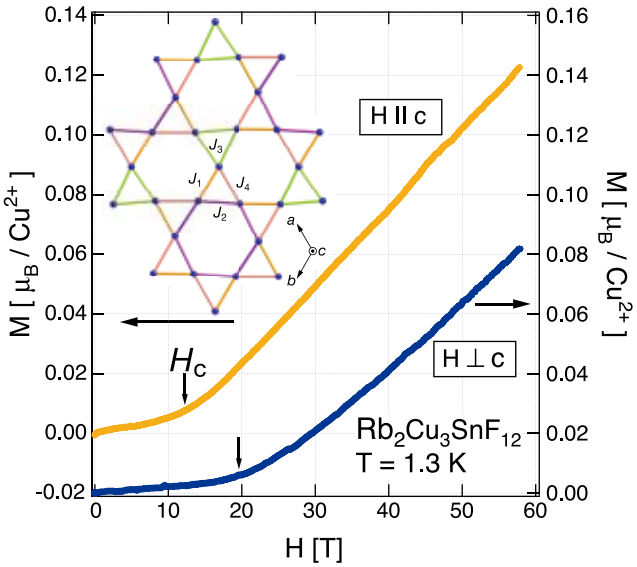

Fig. 1. Magnetization curves of $Rb_2Cu_3SnF_{12}$ for the field directions $H||c$ (left axis) and $H \perp c$ (right axis) measured at T=1.3K. Inset shows the network of the nearest-neighbor exchange interactions between magnetic Cu^{2+}-ions (blue circles) in the ab-plane. The exchange bonds are classified into J_1~J_4.

References

[1] Ch. Waldtmann *et al.*, Eur. Phys. J. B **2**, 501 (1998).
[2] M. Mambrini and F. Mila, Eur. Phys. J. B **17**, 651 (2000).
[3] M. Rigol and R. R. P. Singh, Phys. Rev. Lett. **98**, 207204 (2007).
[4] G. Misguich and P. Sindzingre, Eur. Phys. J. B **59**, 305 (2007).
[5] K. Morita *et al.*, J. Phys. Soc. Jpn. **77**, 043707 (2008).

Authors

K. Morita[a], T. Ono[a], H. Tanaka[a], Y. Narumi, and K. Kindo
[a]Department of Physics, Tokyo Institute of Technology

International Conferences and Workshops

Foundations and Applications of the Density Functional Theory (FADFT)

July 19 -August 10, 2007
O. Sugino and Y. Takada

The FADFT consisted of the workshop part (19-31 July and 6-10 August) and the symposium part (1-3 August). In the workshop two pedagogical lectures were provided everyday and after the lectures significant discussion was done between the lecturers and junior researchers. On average 20-30 attended the workshop in spite of the hot and humid summer. In the symposium, thirty three invited talks and twenty three posters presentations were given to survey the frontiers of this research field. 120 attended the symposium.

FADFT was the second of the ISSP international mini workshop/symposium, which is held annually by the theory division of ISSP. This time, focus was given to the foundations and the applications of the density functional theory (DFT). FADFT was co-chaired by Osamu Sugino and Yasutami Takada. It was sponsored by The Institute for Complex Adaptive Matter (I2CAM), 21st Century COE Program "Quantum Extreme Systems and Their Symmetries" of the University of Tokyo, and Grant-in-Aid for Scientific Research in Priority Areas, "Development of New Quantum Simulators and Quantum Design - A01 Group -" of MEXT.

The topics selected were

(A) Strongly correlated systems
- Combined DFT and may-body theories (e.g. LDA+U and GW+DMFT)
- Many-body theories beyond DFT (e.g. Quantum Monte Carlo and trans-correlated method)
- Efforts to construct new exchange-correlation functionals within/beyond local density approximations (LDA)

(B) Excited states
- Time-dependent version of DFT (TDDFT)

(C) Simulations
- New algorithms for supercomputers, including the order-N algorithms
- Soft and nano materials
- Electronic transport and quantum dynamics of electrons and/or nuclei.

Details on the symposium can be seen in the web site http://www.issp.u-tokyo.ac.jp/public/fadft/. The ppt files and the lecture movies are available on the web site http://www.issp.u-tokyo.ac.jp/public/fadft/program.html, and http://www.issp.u-tokyo.ac.jp/public/fadft/pict_mov.html, respectively.

2nd International Workshop on Protonics and Nano-Interface of Coordination Chemistry, IWPNICC 2008

March 10-11, 2008
O. Yamamuro and H. Kitagawa

The energy problem is one of the most important scientific problems of the 21st century. In the such social situation, the role of hydrogen with energy storage and energy conversion functions is becoming more and more significant in the world. The first purpose of this workshop is to discuss structural and dynamical properties of proton conducting and storage materials in their bulk state and at interfaces. Another purpose of the workshop is to discuss the development of new proton conducting and storage systems and their functional nano-layer integrated systems. In the workshop, eight foreign (from six countries) and nine domestic researchers were invited and gave interesting talks on the above topics. The total number of participants was about sixty.

In the workshop, it was confirmed that the neutron is a powerful prove for hydrogen systems since it has large scattering cross section and reflectivity for hydrogen atoms and exhibits striking contrast for H and D atoms. It is also suggested that synchrotron radiation X-ray, NMR, and thermal experiments are also useful and their combination is very effective to investigate the physical properties of proton-containing systems. It was remarkable that a variety of new proton conducting materials and nano-porous materials have been produced recently in the field of coordination chemistry. Theoretical and computer simulation works are helpful for designing such new materials and understanding the microscopic electrocatalytic reactions at electrode interfaces.

This workshop was financially supported by Japan Science and Technology Agency (JST), Core Research for Evolutional Science and Technology (CREST) Program: Development of the Foundation for Nano-Interface Technology. The management of the workshop was performed by the research stuffs, secretaries, and students of H. Kitagawa laboratory (Kyushu University), S. Kitagawa laboratory (Kyoto Universty), and Yamamuro laboratory (ISSP).

ISSP Workshops

New Developments in ESR of Strongly Correlated Systems

May 21-23, 2007

M. Oshikawa, M. Hagiwara, H. Kikuchi, S. Miyashita, H. Nojiri, and H. Ohta

Electron Spin Resonance (ESR) is one of the most fundamental experimental probes in condensed matter physics. However, perhaps its potential has not been fully utilized in research of strongly correlated systems yet. This is primarily owing to difficulties in the theory of ESR of strongly correlated systems and thus in the interpretation of experimental data. However, recently, reliable analytical and numerical approaches that include correlation effects have been developed in one dimension. With the steady advancement of material synthesis and experimental techniques on the other hand, at this workshop we had intensive discussions on the present status and future directions of the field.

Thanks to the support from the University of Tokyo COE 21 program "QUESTS" , we could have 8 invited speakers from abroad. As a consequence, this workshop is organized as an international workshop and all the presentations were given in English.

Although the subject of the workshop was quite limited, total number of participants over 3 days was as many as 126, with 26 oral and 9 poster presentations. Lively discussions were held in a relaxed atmosphere.

Among the presentations, there was a report of new experiments which reexamine a 20 years old result. This reminded us that there are many interesting, long-standing questions in the field.

Details on the workshop can be found in the web page: URL http://oshikawa.issp.u-tokyo.ac.jp/esr/indexj.html

New Opportunities in Materials Science Using High Brilliance Soft X-ray

July 5-6, 2007

A. Kakizaki, T. Miyahara, H.Daimon, M. Oshima, S. Shin and I. Matsuda

The Synchrotron Radiation Research Organization of the University of Tokyo has started to construct a new undulator beamline at the SPring-8, which will be available in a year or two. The aim of the workshop is to overview the recent topics and developments in the materials science using synchrotron radiation and to discuss on the scientific opportunities which will be available at the new beamline at SPring-8. After a brief talk on the new undulator and beamline at SPring-8, participants including many young scientists discussed on the new scientific opportunities utilizing nano-focusing and/or pico-second time structure of high brilliance undulator light. They discussed on soft X-ray diffraction experiments to investigate characteristics of hidden surfaces and interface, soft X-ray emission spectroscopy of bio-materials, time-resolved experiments of chemical reactions and nano-magnets, etc. New proposals such as STM imaging and photoelectron diffraction experiments were also discussed. In the workshop, synchrotron radiation facilities, UVSOR, KEK-PF and SPring-8, reported on the present status of the light sources and their future plans.

Foundations and Applications of the Density Functional Theory (FADFT)

August 1-3 , 2007
O. Sugino and Y. Takada

This ISSP workshop was held as a part of the international workshop of the same title. See the section of “International Conferences and Workshops”.

Novel Low Temperature Pressure-Induced Phenomena and Current and Possible Pressure Techniques

October 10-12, 2007
K. Murata, K. Shimizu, H. Takahashi, G. Oomi, and Y. Uwatoko

The purpose of this workshop is to discuss the pressure-induced novel phenomena, superconductivity, magnetic order, metal-insulator transitions, etc, and to exchange the latest pressure techniques applied to various sort of experimental physics.

In three days, 30 oral and 29 poster presentations were given. Moreover, the number of participants was 154, which is far beyond the organizer’s expectation and is a proof of high-level interests in these subjects among many researchers. Actually, during the sessions as well as at the coffee breaks, hot discussions were going on all the time. The workshop concluded with many outcomes of new phase diagram under pressure as well as possible and/or realizing new pressure techniques, which have stimulated not only the experimental but also theoretical physicists.

http://www.issp.u-tokyo.ac.jp/cgi-bin/detail.cgi?c=short_term_society_table::132

Present Status and Prospects of Low Temperature Scanning Tunneling Microscopy

October, 12-13, 2007
H. Fukuyama, N. Nishida, T. Hanaguri, F. Komori, and Y. Hasegawa

Technologies on scanning tunneling microscopy (STM) have been rapidly developed since its invention, and now It is used for many materials under various conditions. The application has been extended to wide-ranging research fields, and specifically, low-temperature STM has been utilized for researches in surface science, superconductivity, semiconductor materials, magnetism etc. Although common experimental techniques are used, however, there have been few chances to hear talks of other fields and share the knowhow since researchers present their results at different societies / sections. In this seminar, 98 researchers and students who perform researches with low temperature STM got together, introduced a state-of-the-art research in each field mutually and exchanged the technical knowhow through 24 oral and 14 poster presentations and subsequent discussion. Presentations on surfaces, superconductivity, mesoscopic physics, and local optical response were provided. The seminar was very fruitful since stimulus discussion promoted mutual understanding among researchers of various fields.

Progress in Computational Physics

November 1-2, 2007
N. Kawashima, N. Furukawa, S. Tsuneyuki, Y. Tomita, and T. Suzuki

While continuous advancement of computer-hardware technology is a strong driving force of modern computational sciences, recent important developments are largely due to new computational methods and softwares. At the supercomputer center (SCC) of ISSP, we are accepting approximately 200 new proposals annually from many institutions in Japan, with the aim at developing new algorithms and methods in condensed matter physics. The proposals are classified into three categories: (1) the first-principles calculations of states of matters, (2) strongly-correlated quantum systems, and (3) complex and non-linear systems. In order to clarify the current state of these fields and motivate further investigations, we invited most active researchers, including heavy users of the facilities of SCC, ISSP, and organized the workshop. In particular, we invited four researchers to give prenary lectures: Y. Morikawa (Osaka), M. Sasaki (Tohoku), S. Watanabe (Tokyo), and H. Kontani (Nagoya). The first day was focused on the first principles calculations and the second on the strongly-correlated systems and the complex and non-linear systems. We had totally 80 participants and 44 presentations (30 oral and 14 poster). The talks and discussions represented the high quality of the activities of the community. In addition, we had a special session for discussing our possible actions towards the next-generation supercomputer project (“10-peta-flops project”) of MEXT, Japan.

Frontiers of Physical Chemistry 2007

November 20-22, 2007
J. Yoshinobu

Since the inception of The Institute for Solid State Physics in 1957, several chemistry-based groups have been engaged among more than 40 research groups. So far the collaboration between physicists and chemists has given unique outstanding achievements in condensed matter science. In this workshop the present frontiers of physical chemistry and chemical physics in condensed mater were reviewed. In particular, six subjects were focused: (1) interplay between light and materials, (2) physical properties of nm-scale and low-dimensional materials, (3) dynamics in amorphous and liquid materials, (4) synthesis of exotic materials and their properties, (5) self-organization in soft matter and (6) development and application of new materials. In addition, Professor Emeritus Inokuchi gave a special lecture about solid state organic materials in commemoration of his 2007 Kyoto Prize.

Creation and Destruction of Coherence of Light with Short Wavelength and Those in Materials

November 26-27, 2007
T. Miyahara, M. Aihara, T. Suemoto, and S. Watanabe

In this workshop were discussed various aspects of coherence of light and collective motions in a material interacting with radiation. Creation of higher order coherence is nontrivial in a material system because of the presence of some decohering mechanisms. Many experimental results were shown to indicate that in most cases the coherent motion of elementary excitations are caused by an incoherent pulses much shorter than the period of oscillation. Also the substantial time was devoted to the issues about the Berry phase, quantum entanglement, and potential methods to control the phase of motions in a material. The basic concepts of “energy relaxation” , “phase relaxation” , and “decoherence” were extensively discussed unifying different terminology used in different groups. Some participants proposed future plans to clarify some unsolved or controversial problems, such as the control of gauge phases or the basic assumptions of quantum mechanics and observation.

On the Experimental Apparatuses in the Outstation Project of the University of Tokyo

December 8, 2007
A. Kakizaki, M. Oshima, and S. Shin

The Synchrotron Radiation Laboratory of ISSP has been participating to the Outstation Project of the University of Tokyo and constructing new undulator and beamline at SPring-8. The aim of the workshop is to discuss on the scientific opportunities utilizing high brilliance soft X-ray and to find out a future direction to construct experimental apparatuses at SPring-8. At the workshop, the difficulties and up-to-date experimental techniques were also discussed to handle with the high brilliance soft X-ray from undulator, which inevitably accompany with high heat flux more than 100w/mm^2. Six proposals of the new apparatuses were presented and discussed. The discussion was summarized to suggest that the construction would be stated with the experimental apparatuses for soft X-ray emission spectroscopy of bio-materials, time-resolved experiments of chemical reactions and nano-magnets and photoemission experiments on nana-structure materials. They also recommended a post-focusing mirror system so that many apparatuses designed and constructed for experiments using high brilliance soft X-ray could be connected.

Hydrogen and Water in Condensed Matter

February 4, 2008
J. Yoshinobu

Hydrogen and water are ubiquitous in the universe and on the earth, but their states of existence are still under intensive research. In addition, hydrogen and water play important roles in materials, including proton transfer, hydrogen absorption, catalytic reactions on surfaces, electrochemistry, ice, gel, etc. Recent activities in this field have been growing very rapidly using many different techniques; neutron scattering, synchrotron radiation, ultra-fast lasers as well as first-principles calculations. In this workshop, we reviewed and discussed the present status of hydrogen and water in condensed matter physics and chemistry.